SAND 2007-1923P
Prediction of Arsenic Removal by Adsorptive Media: Comparison of Field and Laboratory Studies

[1]Malcolm Siegel, [1]Alicia Aragon, [2]Hongting Zhao, [3]Shuguang Deng, [4]Melody Nocon, [1]Malynda Aragon

Sandia National Laboratories
Albuquerque, NM

[2]University of Wyoming
Laramie, WY 82071-3354

[3]Department of Chemical Engineering
New Mexico State University
Las Cruces, NM 88003

[4]ENVIRON International Corporation
Tampa, FL

Abstract

Sandia National Laboratories has carried out pilot tests of innovative adsorptive media that have the potential to reduce the costs of arsenic removal from drinking water. Arsenic removal performance of 3 different adsorptive media under constant ambient flow conditions were compared using a combination of static (batch) and dynamic flow tests. These included batch sorption isotherm and kinetic sorption studies, Rapid Small Scale Column Tests (RSSCT), and a pilot test at domestic water supply well. The media studied exhibited contrasting physical and chemical properties and included a granular ferric oxyhyroxide (E33), a granular titanium oxyhydroxide (Metsorb), and an ion exchange resin impregnated with iron oxide nanoparticles ($ArsenX^{np}$). The E33 media gave the best performance based on volume of water treated until breakthrough at the arsenic MCL (10 µg/L or10 ppb) and full capacity at media exhaustion. A main goal of this project is evaluate alternative methods to predict pilot-scale and full-scale performance from laboratory studies. The relative arsenic sorption capacity of the three media could be predicted from the batch sorption studies and RSSCT column results. The Klinkenberg analytical solution gave good semi-quantitative description of arsenic breakthrough curves and pore water profiles in the pilot tests based on parameters obtained in the RSSCT studies. The model is potentially useful for scaling up adsorptive media performance to any reasonable size from the data obtained in laboratory studies. These results may be useful to communities that cannot afford to carry out expensive pilot tests of multiple media, especially if other information about backwash requirements and costs (capital and labor) for full-scale systems are already available.

1.0 INTRODUCTION

1.1 Purpose

The Arsenic Water Technology Partnership (AWTP) is a collaborative program involving the American Water Works Association (Awwa) Research Foundation, Sandia National Laboratories (SNL), and WERC (A Consortium for Environmental Education and Technology Development) (Siegel et al. 2005). As a member of the AWTP, SNL is conducting pilot scale evaluations of the performance and cost of innovative drinking water treatment technologies aimed at meeting the new arsenic maximum contaminant level (MCL) of 10 µg/L (effective January 2006). The costs of the new drinking water standard will be born disproportionately by small communities in the rural Southwestern United States that lack the technical and financial resources to carry out pilot tests needed to choose the best technology for their water system. The communities will be further challenged to pay for the costs of construction and maintenance of the water treatment systems and must choose the most cost-effective technology. One of the objectives of this study is to determine the most efficient way to predict the absolute and relative sorption capacities of different candidate adsorptive media so that the most appropriate technology can be selected for community water systems.

Arsenic is removed in fixed bed filtration via adsorption, the physical and chemical attachment of the adsorbate (arsenic) to the surface of the adsorbent media grains. The removal capacity and effectiveness of the arsenic removal media are dependent on a number of physical and chemical factors. Chemical factors include the strength of the chemical bond between the arsenic and the adsorbent, the kinetics of the adsorption reaction, the concentrations of ions competing for sorption sites, the concentration of arsenic in the feed water, and the pH of the feed water. Physical (transport) factors include the effective surface area, which is a function of the accessibility of the porosity of the media grains; steric factors affecting the accessibility of the pore sites by arsenic ions; and the time available for arsenic ions to migrate to pore sites. This last property is related to the flow rate of the feed water that conveys the arsenic into the bed of adsorbent media.

Prediction of arsenic removal from a packed column is very challenging due to the following reasons:

1) the extremely long breakthrough time for "good" adsorbents with high As capacity;
2) a lack of accurate adsorption equilibrium and kinetics data at low As concentration;
3) fluctuations of influent As concentration and other water chemistry during breakthrough tests;
4) fluctuation and scattering of As analysis results;
5) variation of adsorbent properties during the prolonged breakthrough test; and
6) variation of the arsenic concentration front inside the column with time.

In this study, the arsenic removal performance of 3 different adsorptive media under constant ambient flow conditions was compared using a combination of static (batch) and dynamic flow tests. These included batch sorption isotherm and kinetic sorption studies, Rapid Small Scale

Column Tests (RSSCT), and a pilot test at a community groundwater supply source. The media studied exhibited contrasting physical and chemical properties and included a granular ferric oxide (E33), a titanium oxide (Metsorb), and an ion exchange resin impregnated with iron oxide nanoparticles ($ArsenX^{np}$). In order to understand and potentially predict the transport of arsenic through the media at laboratory and pilot test scales, some basic mineralogical and surface chemical analyses were carried out. These included XRD (X-ray diffraction), SEM/EDS (Scanning Electron Microscope/Energy Dispersive Spectroscopy), and surface area analysis by the Brunauer, Emmett and Teller (BET) measurement technique. In addition, physical properties that might affect the hydraulic performance of the media during the test were examined. Post – test data was obtained from the pilot test of the granular ferric oxides (E33) media including arsenic concentration profiles in the pore water.

A main goal of this project is to develop an effective but simple modeling tool to predict pilot-scale and full-scale performance from laboratory studies and provide guidance for arsenic removal process development, scale-up and design. Data were collected in order to compare the abilities of experimental methods and a theoretical analytical solution to describe the arsenic removal and transport. The analytical solution (Klinkenberg analytical solution) could be programmed on a simple spreadsheet to compare to arsenic breakthrough curves and the pore water profiles in the pilot tests.

2.0 MATERIALS AND METHODS

2.1 Water composition

Socorro Springs in Socorro, New Mexico, was the first demonstration site to be selected in a multiyear pilot demonstration sponsored by the Arsenic Water Technology Partnership. The sources of the water supply are Socorro and Sedillo Springs located in the foothills west of the City of Socorro. Water from both springs is mixed slightly down gradient of the spring boxes, followed by a shutoff valve. Below the shutoff valve, an eight-inch subsurface, carbon steel line delivers approximately 540 gpm water via gravity to the chlorination building where the water is disinfected and oxidized using chlorine gas injection just prior to storage in the Springs Site Storage Tank. During this pilot, a portion of the chlorinated Springs Site water was diverted to the arsenic adsorption media filters, which were located inside the Springs Site chlorination building. The treated water and backwash wastewater from the arsenic adsorption media filters were discharged to an on-site subterranean infiltration gallery via a 2-inch polyethylene pipe. The total discharge was limited to 3 gpm or less; none of the treated water was returned to the drinking water distribution system.

A representative analysis of the Springs Site raw water quality is presented on Table 1. The water has moderate levels of silica, sulfate, and hardness and is near neutral in pH. The arsenic level ranges from four to five times the January 2006 MCL of 10 µg/L (10 ppb).

2.2 Adsorptive media

The three adsorptive media discussed in this paper were part of a larger set of 5 adsorptive media tested at Socorro Springs between January and July 2005 in Phase I of the Socorro Springs Pilot Test. Technologies were considered based primarily on the results of the 2003 and 2004 Vendor Forums held in October of each year at the New Mexico Environmental Health Conference (Siegel et al. 2006b). The selection process is described the Forum website: **http://www.sandia.gov/water/arsenic.htm**. The ArsenX^{np} hybrid resin was supplied by the Purolite Company. Graver Industries (formerly Hydroglobe) supplied the granlar TiO_2 Metsorb media and Adedge supplied the E33 media, a granular ferric oxide. The companies were responsible for providing quality-controlled media and information regarding suggested pilot system design and operational parameters. The pilot test is described in a later section below. Purolite, Adedge, and Hydroglobe indicated that no pretreatment was required for their respective arsenic adsorption media.

Note that the use of the media in the tests does not imply any endorsement of the product by Sandia National Laboratories. In addition, it is important to recognize that the performance of the media in the tests in 2005 may not be indicative of the performance of other media manufactured by the companies at later dates.

Table 1. Nominal Socorro Water Quality.

Parameter	Chlorinated Feed Water
Conductivity (µS/cm)	356-360
Temperature (degrees Celsius)	30.1-30.5
Free chlorine (mg/L as Cl_2)	0.5 – 0.8
pH	7.9
Iron (ppb)	38.2
Total Arsenic (ppb)	42.9
Speciated Arsenic	
Particulate (ppb)	1.9
As(III) (ppb)	2.1
As(V) (ppb)	40.9
Titanium (ppb)	ND (0.38)
Zirconium (ppb)	ND (0.22)
Alkalinity (ppm)	NA
Nitrate (ppm)	0.4
Calcium (ppm)	17.4
Magnesium (ppm)	4.1
Sodium (ppm)	57.1
Silica (ppm)	24.9
Aluminum (ppb)	23.2
Vanadium (ppb)	11.3
Gross Alpha/Beta (pCi/L)	Alpha-6.50, Beta-3.52
Chloride (ppm)	12.1
Fluoride (ppm)	0.5
Phosphate (ppm as PO_4)	0.034
Sulfate (ppm)	28.4
Total Organic Carbon (TOC)	0.5

ppm = parts per million; ppb = parts per billion
NA = not available; ND = not detected above method detection limit (MDL is given)

Bulk Physical Properties

Figures 1a – 1c show scanning electron micrographs of the media; Table 2 describes their bulk physical properties. The E33 and Metsorb media were delivered dry; the ArsenX^{np} beads were delivered wet. All media were ready to load into SNL adsorption columns upon receipt. The volume, weight, and height of each of the media loaded into adsorption columns were recorded at several points in time: initial, after transport to the Socorro Springs site, after backwashing (BW), after additional media was added, and at the start of the pilot. This information is summarized in Siegel et al. (2007).

An indirect measure of the physical durability of the media was obtained by examining the change in the size distribution resulting from shipping and handling prior to loading of the media into the columns. The percentage of media smaller than the smallest particle size fraction declared by the vendor was calculated. This resulting percentage is the attrition loss; percentages for these 3 media ranged from 0.8% to 13% (see North 2006). For example, 13% of the E33 media was smaller than 35 mesh, whereas the vendor declared range of sizes was 10 x 35; therefore a 13% attrition loss was determined for the E33. However, some error resulted from

the use of a No. 40 sieve instead of a No. 35 or No. 32 sieve (0.425 mm instead of 0.500-0.600 mm), which is the size specified by the vendor (Adedge). For comparison, attrition losses for other media examined in the more comprehensive study (North 2006) ranged from 0.8 to 32.2%.

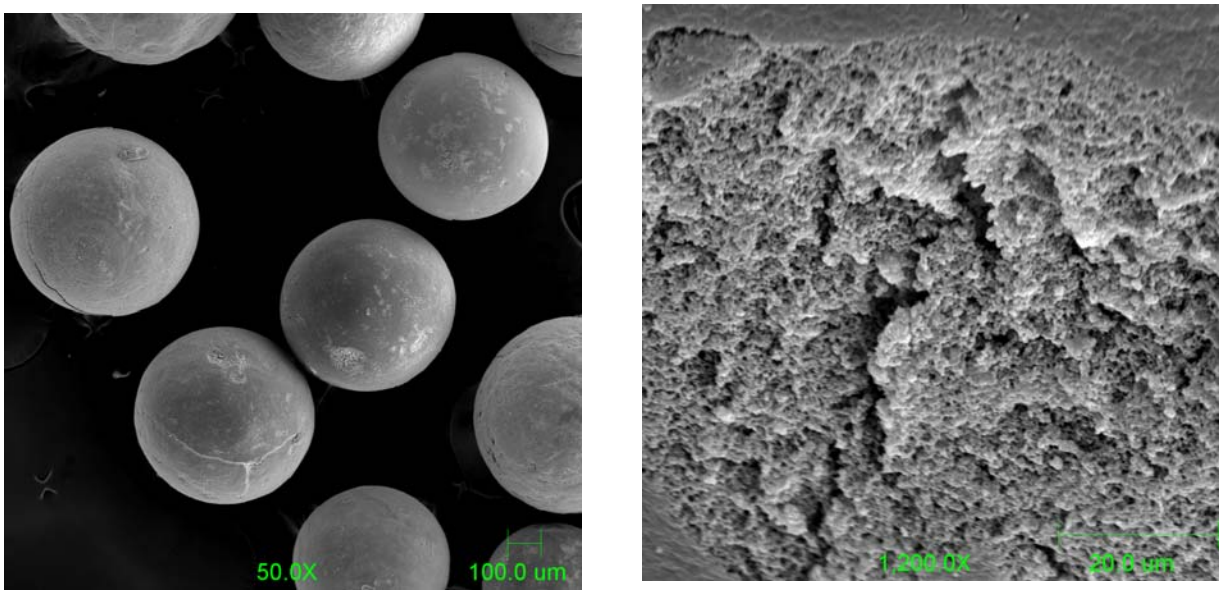

Figure 1a. SEM Photos of ArsenX^{np} Media (50x and 1200x magnification).

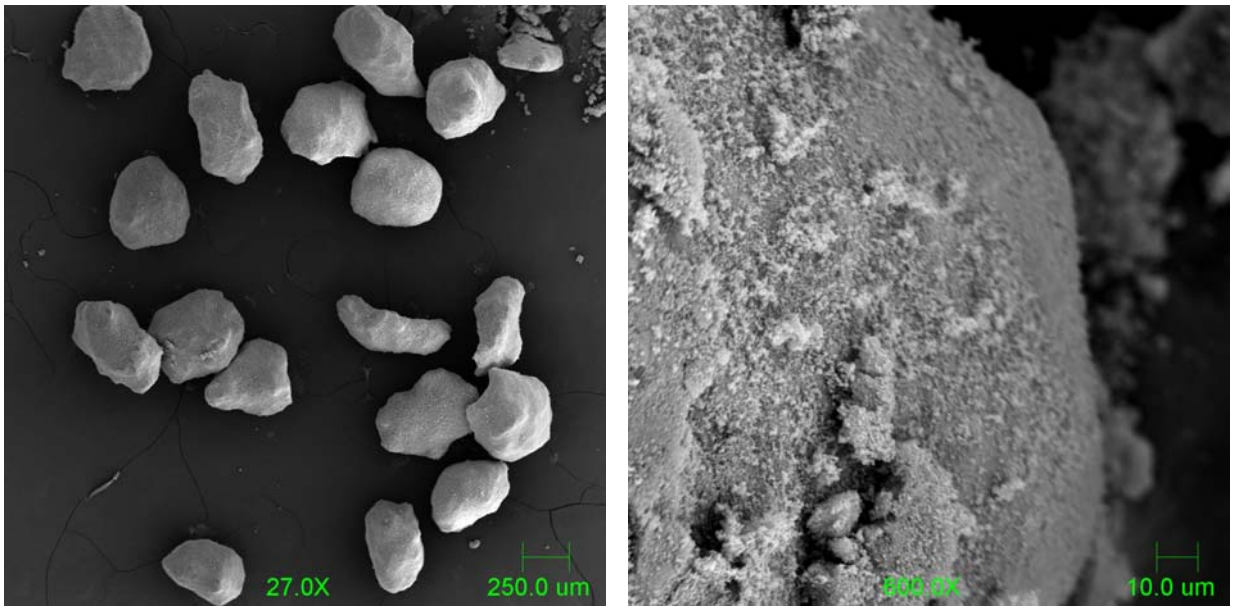

Figure 1b. SEM Photos of Metsorb Media (27x and 600x magnification).

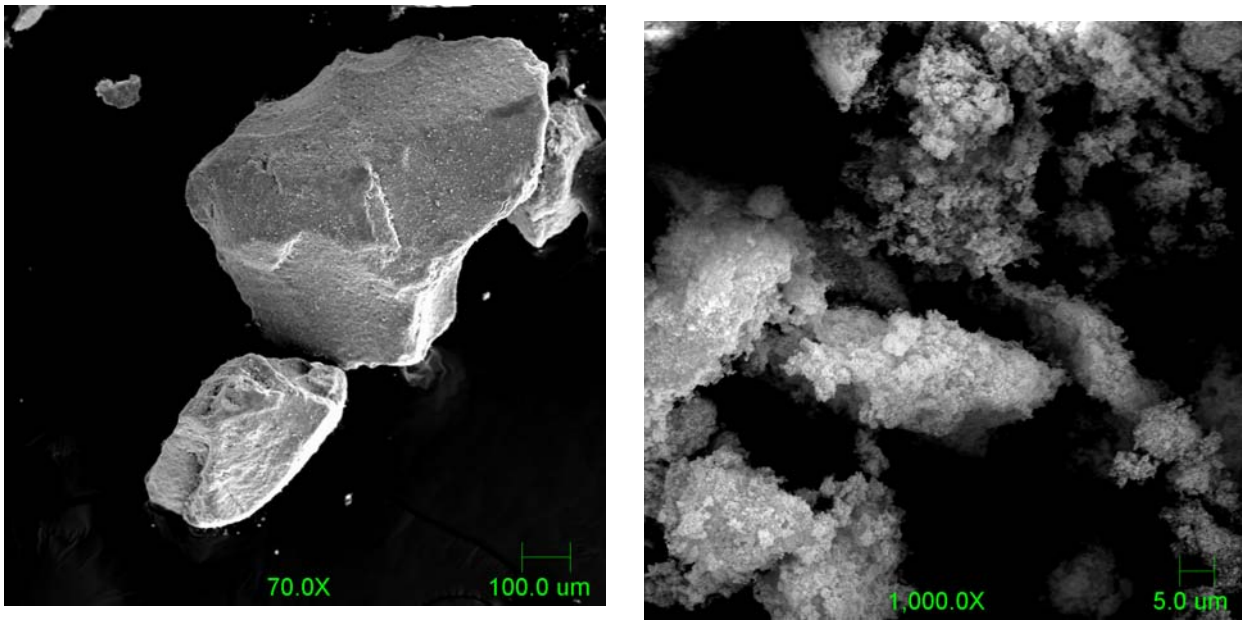

Figure 1c. SEM Photos of E33 Media (70x and 1000x magnification).

The uniformity coefficient is $C_u = D_{60}/ D_{60}$ where D_{60} is the weight of the grain size that is 60 percent finer and D_{10} is the weight 10 percent finer on the grain size distribution curve. Lower values of the C_u indicate well-sorted media. Such material will have favorable hydraulic properties because there will be few fine grain particles mixed with larger particles to clog the system. The ArsenX^{np} had the lowest uniformity coefficient, consistent with visual observation of the uniform nature of the resin beads (Fig. 1a).

All of the media experienced minor compaction (less than 2% difference from initial height) during transport to the site and required additional media to meet design height requirements. Most of the media swelled after water was added and the columns were backwashed. During operation, it was observed that media compacted as much as 2 to 5 inches in some of the columns. It is somewhat unexpected to see no increase in pressure drop across each of the columns. As discussed in Siegel et al. (2007), this may have been due poor column design or that the pressure gauges could have been inaccurate and/or malfunctioning when in use.

Table 2. Bulk Properties of Media.

Media	Metsorb	ArsenX^{np}	E33
Chemical Constituents	Nano-crystalline titanium dioxide	Nanoparticle selective resin with iron oxide as the functional group	Iron oxide/ hydroxide
Physical appearance	White granular beads	Reddish-orange resin beads	Amber granules
Bulk density (lb/ft^3)	50	49 - 52	30
Sieve sizes, US std.	16 x 60	16 x 50	10 x 35
Particle size (mm)	1.18 x 0.25	1.18 x 0.3	0.5 x 2.0
Attrition loss (%)	0.8	0.8	13
Uniformity Coefficient C_u	1.97	1.64	2.44

Mineralogical and chemical studies

Methods

XRD analyses were performed on a Bruker D8 Advance X-Ray Diffractometer using CuKa radiation, a step size of 0.05º and step time of 1 s, operated at 40 kV and 30 mA. The samples were ground to fine particles and dispersed using deionized water on a glass slide and dried at room temperature before analysis.

SEM/EDS data were collected on a JEOL JSM-6300V Scanning Microscope with energy dispersive capabilities operated at 20 kV. Powder samples were mounted directly on carbon conductive tabs and sputter-coated with gold (or carbon) before analysis.

BET surface area and pore size distribution were measured using QuantaChrome Autosorb-6B Analyzer (Quantachrome Corporation). The samples were degassed at 120ºC for ~12 hours (or 30ºC, ~24 hours for ArsenX^{np}). Surface areas were determined using the BET equation on 5-point N_2 gas adsorption isotherms, and the pore-size distributions were obtained from the desorption branches using the standard Barrett-Joyner-Halenda (BJH) method without further correction (Barrett et al. 1951).

Results

Table 3 summarizes the results of the SEM/EDS, BET and XRD studies. E33 and ArsenX^{np} have the lowest BET surface areas and largest average pore diameters. Figures 2 and 3 compare the differential pore size and cumulative pore volume distributions of the different media. The pore size distribution curves show the range of pore sizes and the peaks indicate the dominant pore size. In the differential pore size distribution curve (Figure 3) the y-axis, Dv (logD), is the derivative pore volume divided by the derivative of the log value of pore diameter. The majority of the pore volumes of E33 arise from pores with diameters of 400 to 700 Å (mode ~ 600 Å). Metsorb has a higher diameter dominant pore size range of ~ 500 to 800 Å (mode ~ 700Å). Possible shrinkage of the resin during the degassing process as well as the presence of volatile compounds may contribute to the observed characteristics of ArsenX^{np}.

Table 3. Summary of Analyses of Arsenic Adsorption Media.

Media	BET Surface Area (m^2/g)	Average Pore Diameter (Å)	Total Pore Volume (TPV) (cm^3/g)	Constituents (XRD)	Dominant Elements (EDS)
Metsorb	211	64	0.34	Crystalline TiO_2 (*Anatase*)	Ti, O
ArsenX^{np}	120	174	0.05	Amorphous iron oxide/hydroxide	Fe, O, C
E33	147	245	0.90	Iron oxide/hydroxide (*Goethite*)	Fe, O

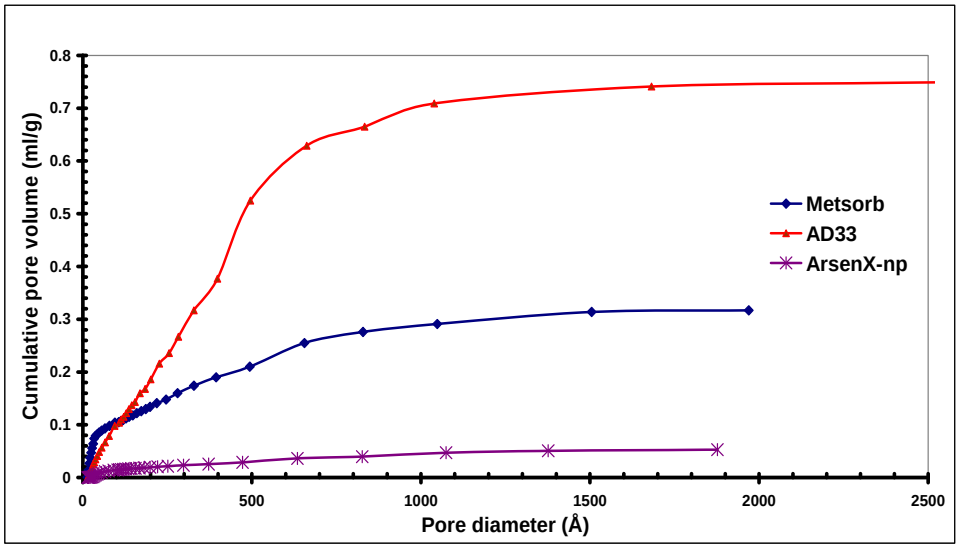

Figure 2. Cumulative Pore Volume Distributions for Three Adsorbent Media

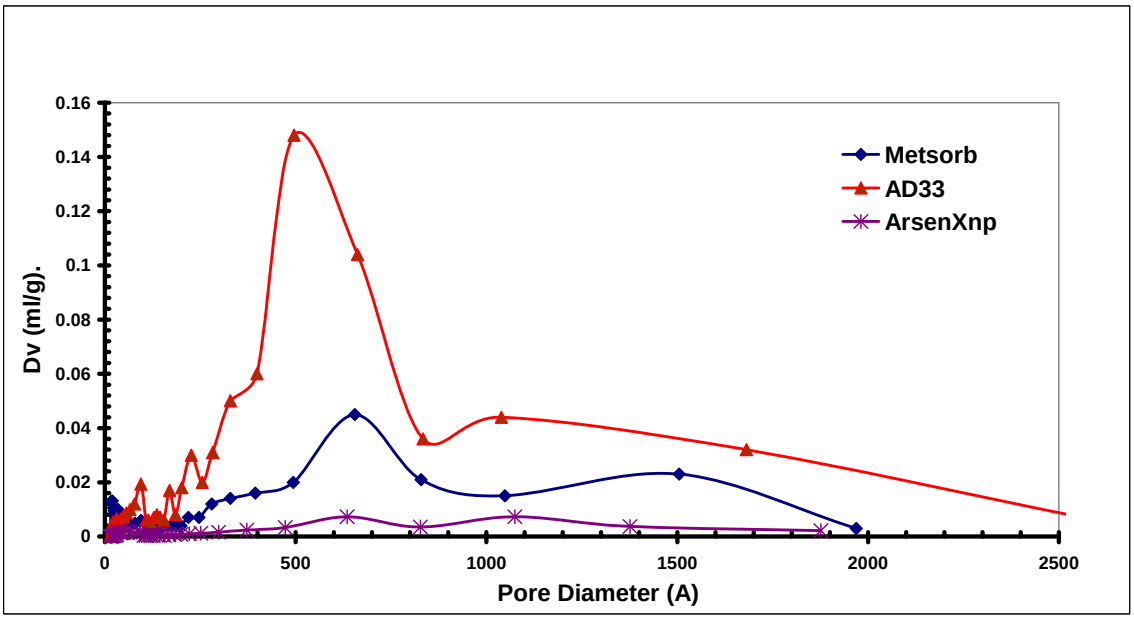

Figure 3. Pore Size Distributions for Three Adsorbent Media.

3.0 SORPTION STUDIES

3.1 Adsorption Kinetics in Socorro Springs Water

Batch kinetic sorption studies were carried out to determine an appropriate reaction time for establishing equilibrium conditions in the development of sorption isotherms, to measure chemisorption rates and to extract effective diffusivities for mass transfer. Another objective was to determine if sorption rates at room temperature (about 15°C) differed appreciably from those at the water temperature expected in the pilot test (about 40°C).

Materials and Methods

The E33 and Metsorb media were ground and washed with deionized water to obtain 325 x 400 mesh; the ArsenX^{np} resin was used as received. Adsorption kinetic studies were carried out using 0.20 or 0.01 g samples (0.20 g for ArsenX^{np}) in 1000 mL arsenic-doped Socorro groundwater at 15 or 40ºC using a temperature-controllable water bath. The doped Socorro waters were prepared by mixing ten liters of the Socorro groundwater (nominal arsenic concentration of 44 µg/L) with 660 µL of a 1000 ppm arsenic stock solution to produce a solution with a nominal arsenic concentration of 110 µg/L. The water sample was put in a 1500 mL double-layered glass jar with the water from water batch flowing through the spacing between the layers. The temperature of the water was monitored to reach to 15ºC or 40ºC before adding the sorbents. Aliquots of the sample (~5 mL) were collected at around 2, 5, 15, 30, 60, 120, 240, 480, 600, 1440, 1680 and 1920 minutes using a 10-mL syringe and filtered through GHP Acrodisc 0.2-µm syringe filters. The water samples were then assayed for arsenic concentration using inductively coupled plasma mass spectrometry (ICP-MS).

Results

Figures 4 through 6 show the kinetics of arsenic adsorption on the media tested in Socorro groundwater. The results suggest that arsenic adsorption in Socorro groundwater under the selected experimental conditions was rapid. The results show that a 24-hour equilibration period (1440 minutes) should be sufficient to establish steady state or equilibrium for sorption experiments using similar particle sizes and initial arsenic concentrations. This information was used in designing the sorption isotherm experiments described in the next section.

Data Analysis to Obtain Chemisorption Rate Constants

For many adsorption processes occurring on heterogeneous materials, it has been found that chemisorption is the rate-controlling step (Reddad et al. 2002; Ho and McKay 1998, 2000). Such processes can be described with a pseudo-second-order kinetic equation in which the reaction rate is dependent on the concentration of sorbed species and the equilibrium concentration of the sorbed species. The pseudo-second-order kinetic rate equation can be expressed as (Ho and McKay 1998, 2000; Reddad et al. 2002):

$$dQt/dt = k(Q_{eq} - Q_t)^2 \qquad \text{(Eq. 1)}$$

where Q_{eq} (mmol As/g media) is the sorption capacity at equilibrium; Q_t (mmol As/g media) is the solid-phase loading of arsenate at time t; and t is time (min). The k (g/mmol∗min) is the pseudo-second-order rate constant for the kinetic model. Considering the boundary conditions of $Q_t = 0$ (at $t = 0$) and $Q_t = Q_{eq}$ (at $t = t_{large}$), the following linear equation can be obtained:

$$t/Q_t = 1/v_o + t/Q_{eq} \qquad \text{(Eq. 2)}$$

$$v_o = k*Q_{eq}^2 \qquad \text{(Eq. 3)}$$

where v_o (mmol/g∗min) is the initial adsorption rate. Therefore, by plotting t versus t/Q_t, the v_o and Q_{eq} values can be determined.

The results were fitted using the pseudo-second-order kinetic model (Eq. 2) to estimate the rate constants, initial sorption rates, and adsorption capacities for arsenate. Relevant parameters are summarized in Table 4. The high fitting coefficients (R^2 ~0.999) indicated that the adsorption of arsenic on the tested media could be well described using the pseudo-second-order kinetic model. Figures 4 to 6 show that approximately 75% to 95% of the initial arsenic in solution (about 110 ppb) was removed by the end of the 24-hr equilibration period. Rate constants and initial adsorption rates decrease in the order: Metsorb > E33 >> $ArsenX^{np}$. E33 showed the highest equilibrium sorption capacity in the kinetic tests. Rate constants were considerably higher at 40°C than at 15°C.

These differences are potentially attributable to differences in the physical and chemical properties of the media (i.e., composition, pore size, surface area, surface charge, arsenic affinity, etc.). The initial rate appears to be related to the mode of the pore size distribution curve rather

than surface area or average pore diameter (Metsorb has highest mode (~ 700 Å) in the differential pore size distribution curve in Figure 3 but relatively lower values of the other parameters.)

Table 4. Kinetic Parameters for Arsenic Adsorption in Socorro Groundwater Using Pseudo-Second-Order Kinetic Model.

Media	Temperature (°C)	R^2	k	V_o ($x10^{-3}$)	Q_{eq} mmol/g	Q_{eq} mg/g
E33	40	0.999	6.08	2.43	0.020	1.50
	15	0.998	3.45	1.38	0.020	1.50
MetSorb	40	0.999	20.54	7.42	0.019	1.42
	15	0.999	5.30	1.91	0.019	1.42
$ArsenX^{np}$	40	0.992	1.03	0.201	0.014	1.05
	15	0.992	0.57	0.111	0.014	1.05

R^2= Model-fitting coefficient;
K = The pseudo-second-order rate constant for the kinetic model (g/mmol∗min);
v_o = Initial adsorption rate (mmol/g∗min);
Q_{eq} = The sorption capacity at equilibrium ($mmol_{As}$/g) or mg/g.

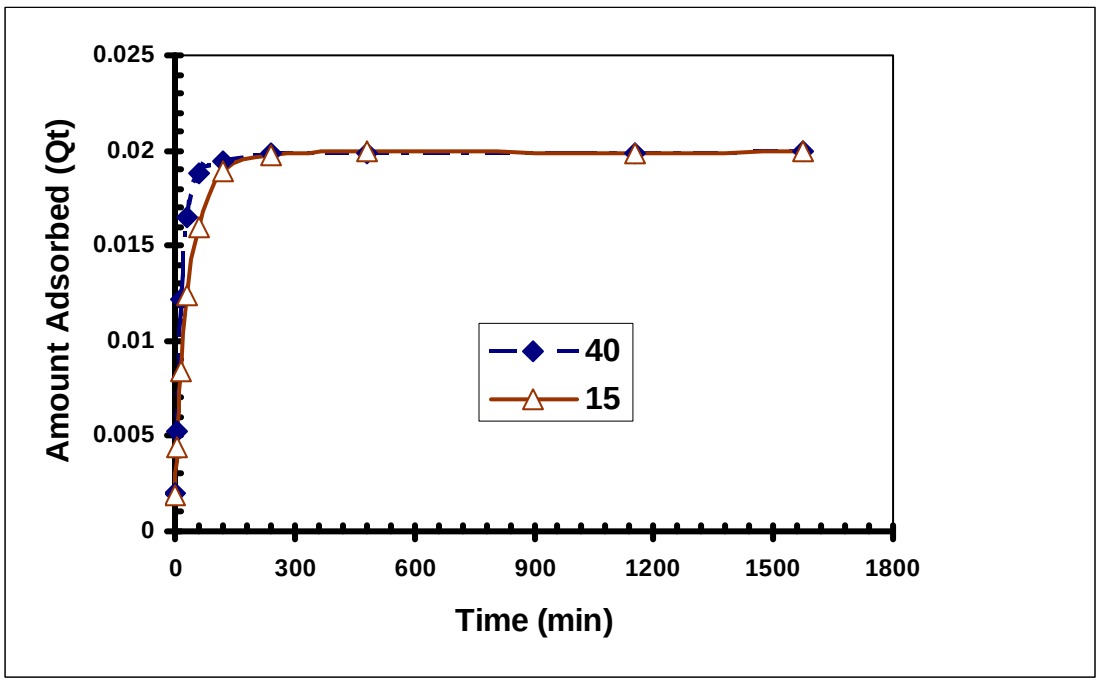

Figure 4. Arsenic Adsorption Kinetic Data for E33 (Qt as mmol As/g) at 15°C and 40°C.

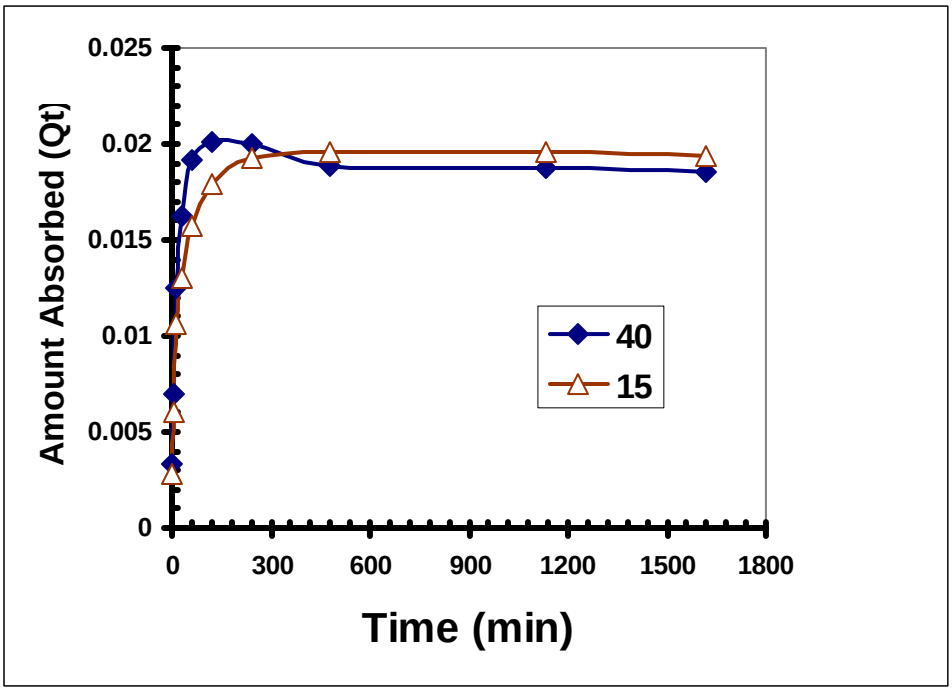

Figure 5. Arsenic Adsorption Kinetic Data for Metsorb (Qt as mmol As/g) at 15°C and 40°C.

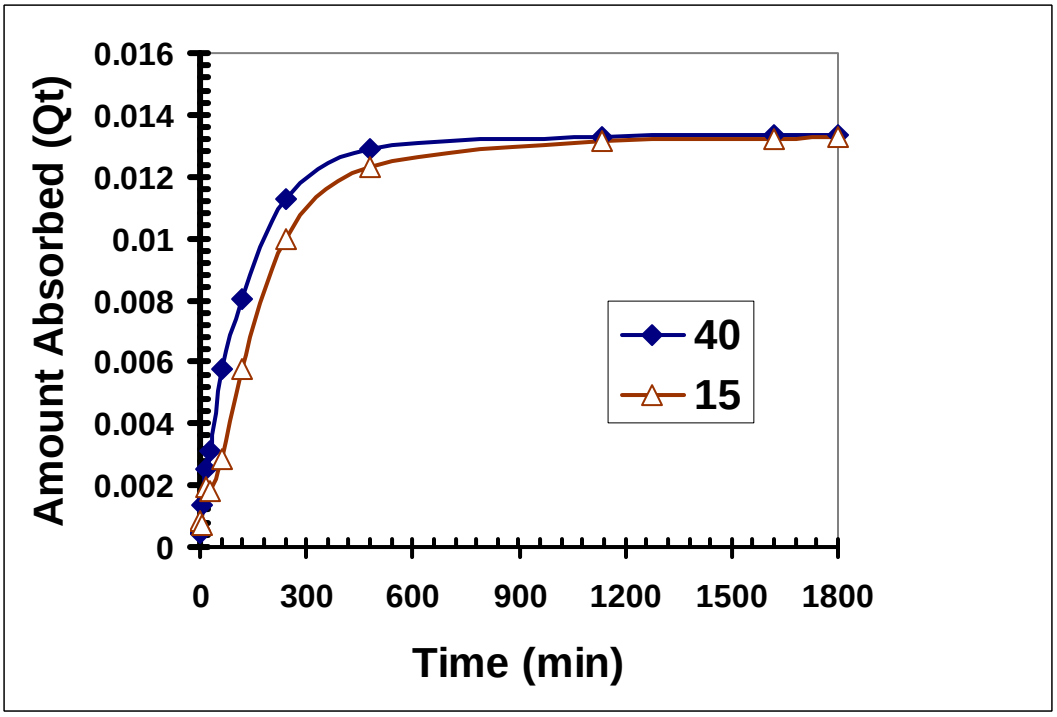

Figure 6. Arsenic Adsorption Kinetic Data for ArsenX^{np} (Qt as mmol As/g) at 15°C and 40°C.

Data Analysis to Obtain Diffusion Coefficients

In order to extract the effective diffusivity of arsenic in the macropores of adsorbent media, a diffusion equation for a macropore-controlled system can be obtained from a differential mass balance on a spherical shell element of the adsorbent particle (Ruthven 1984):

$$(1-\varepsilon_p)\frac{\partial q}{\partial t}+\varepsilon_p\frac{\partial c}{\partial t}=\varepsilon_p D_p\left(\frac{\partial^2 c}{\partial R^2}+\frac{2}{R}\frac{\partial c}{\partial R}\right) \qquad \text{(Eq. 4)}$$

where ε_p is adsorbent particle porosity, q(R, t) is the adsorbed phase concentration (μg/L of adsorbent), t (s) is time, c (μg/L) is the adsorbate concentration in the supernate, D_p (cm^2/s) is the macropore diffusivity of adsorbate in the adsorbent, and R (cm) is the radial distance from the center of the adsorbent particle. The macropore diffusivity (D_p) is assumed to be independent of concentration in the above equation.

Solution of this equation based on that of Crank (1976) and Ruthven (1984) is derived in Appendix 1. For fractional adsorption uptake M_t/M_{max} above 70%, the solution with a 2% error is given by:

$$\frac{M_t}{M_{\max}}\cong 1-\frac{6}{\pi^2}\exp\left(\frac{\pi^2 D_e t}{R_p^2}\right) \qquad \text{(Eq. 5)}$$

Where M_t (μg/L) is the mass gain of adsorbent at time t, M_{max} (μg/L) is the mass gain of adsorbent at infinite time, and D_e (cm^2/s) is the effective diffusivity defined by:

$$D_e=\frac{\varepsilon_p D_p}{\varepsilon_p+(1-\varepsilon_p)K} \qquad \text{(Eq. 6)}$$

where K is the Henry's Law equilibrium adsorption constant. K is equal to K_d x ρ where K_d is the linear adsorption distribution constant (ml/gm) and ρ is the bulk density (gm/ml).

A plot of Ln(1-(M_t/M_{max})) vs. time should generate a straight line with a slope of $\left(\frac{-\pi^2 D_e}{R_p^2}\right)$ and an intercept of $Ln\left(\frac{6}{\pi^2}\right)$, from which the effective diffusivity, D_e, for arsenic diffusion in the macropores of the media can be calculated. $\left(\frac{D_e}{R_p^2}\right)$ is the diffusion time constant (s^{-1}) that measures the diffusion rate of an adsorbate in the porous media. A large diffusion time constant suggests a slow diffusion rate of adsorbate molecules in the porous media.

This solution for the fractional adsorption uptake was used to correlate the adsorption kinetics data described above. The values for effective diffusivity D_e are shown in Table 5 and are calculated based on data points with M_t/M_{max} above 40% assuming an average particle size of

0.035 mm. The diffusivity values (~10^{-10} cm^2/s) are consistent with the literature value of 2.64×10^{-9} cm^2/s for the GFH adsorbent reported by Sperlich et al (2005).

Table 5. Effective Arsenic Diffusivity for Adsorptive Media at 15 C

Media	D_e (cm^2/s)	R^2	Range M_t/M_{max}
E33	2.48 E-10	0.975	0.62 – 1.00
Metsorb	3.72 E-10	0.998	0.54 – 0.99
$ArsenX^{np}$	8.69 E-11	0.994	0.43 – 0.99

3.2 Isotherm Studies

Batch sorption studies were carried out to obtain isotherm parameters to estimate the capacity of the media at different influent concentrations. In general, the media were ground into smaller particles than were used in the pilot test in order to minimize the effects of mass transfer within the grains and thereby reduce the time required to reach steady state. The equilibration times were based on the kinetic studies described in the previous section.

Media preparation and sorption measurements

Raw metal oxide media was ground with a mortar and pestle, placed in a sieve shaker and separated by particle size. Sieve fractions were rinsed with distilled water; and except for $ArsenX^{np}$ were dried at 105°C overnight in an oven; 325 x 400 mesh particles were used for sorption experiments. Titrations with a strong base (1 N KOH) were performed to minimize potential pH drops during the equilibration due to acid residuals present on media surfaces from manufacturing. Five grams of each media sample were placed into a container and enough water was added to create slurry. Initial pH readings of the slurries were typically below pH = 7, and incremental doses of 0.3 mL of potassium hydroxide were added to solution to bring the slurries to a pH between 7 and 8 (bracketing the ambient pH of the utility water). Samples were agitated overnight; if the pH dropped during this equilibration, the titration procedure was repeated. The fully titrated slurries were placed in weighing trays and were air dried under a fume hood for a period of over two days.

Ten one-liter stock solutions with initial arsenic concentrations ranging from ambient concentration (about 44 ppb [44 µg/L]) to 12 ppm (12 mg/L) were prepared from chlorinated water taken from Socorro Springs water utility (Table 1). For each media, a set of ten bottles was filled with approximately 50 mg of media and 40 mL of a specified initial concentration stock solution. Bottles were set in a rotary agitator and sampled approximately twenty-four hours after the beginning of agitation. The solution from each bottle was placed into a centrifuge for separation of the solids from the supernatant. The final pH in each bottle was recorded. Final arsenic concentrations were measured by ICP-MS analysis.

Data Analysis

Figure 7 shows sorption isotherms with Q, the amount of arsenic sorbed (mg/kg), on the y axis and C_{eq}, equilibrium (final) arsenic concentrations (mg/L) on the x axis. Two types of isotherms equations were calculated for each media. An equation for a linear isotherm was calculated from a linear regression of Q and C_{eq}, with the following expression:

$$Q = K_d C_{eq} \qquad \text{(Eq. 7)}$$

where C_{eq} is proportional to Q by a factor K_d (mL/g). A dimensionless K_d value (also known as Henry's law constant) was calculated as $K = K_d\rho$. Values of the bulk density ρ are found in Table 2. Results and goodness-of-fit R^2 values are shown in Table 6. A range of dimensionless K_ds was also calculated as $K = K_d\rho = Q/C_{eq}$ from each measurement over the concentration range studied.

For each media, an equation for a Freundlich isotherm was calculated from the linear regression of the logarithmic plot of Q and C_{eq}, with the following expression:

$$Q=K_F C_{eq}^{nF} \qquad \text{(Eq. 8)}$$

where the slope and the y-intercept of the logarithmic linear regression are equal to n_F and K_F (mL/g), respectively. Results are also shown in Table 6.

Table 6. Results of Isotherm Experiments.

Isotherm	K_d model			Freundlich $Q=K_F C^{nF}$				
Media	**Fitted $K_d\rho$**	**R^2**	**$K_d\rho$ range**	**K_F**	**n_F**	**R^2**	**Q_{10ppb}**	**Q_{40ppb}**
E33	78,400	0.578	67,200 – 690,000	21,000	0.31	0.997	4,970	7,670
ArsenX^{np}	203,000	0.347	173,000 – 655,000	57,000	0.55	0.925	4,630	9.860
Metsorb	95,100	0.831	9,930 -120,000	75,800	0.90	0.937	1,180	4,130

Q=mg/kg; Q_{10ppb} and Q_{40ppb} refer to sorbed concentration at 10 ppb and 40 ppb As C_e in solution, respectively, and were calculated from the isotherm equations. $K_d\rho$ (dimensionless) is also known as Henry's Law constant
K_F = L/kg or mL/g.

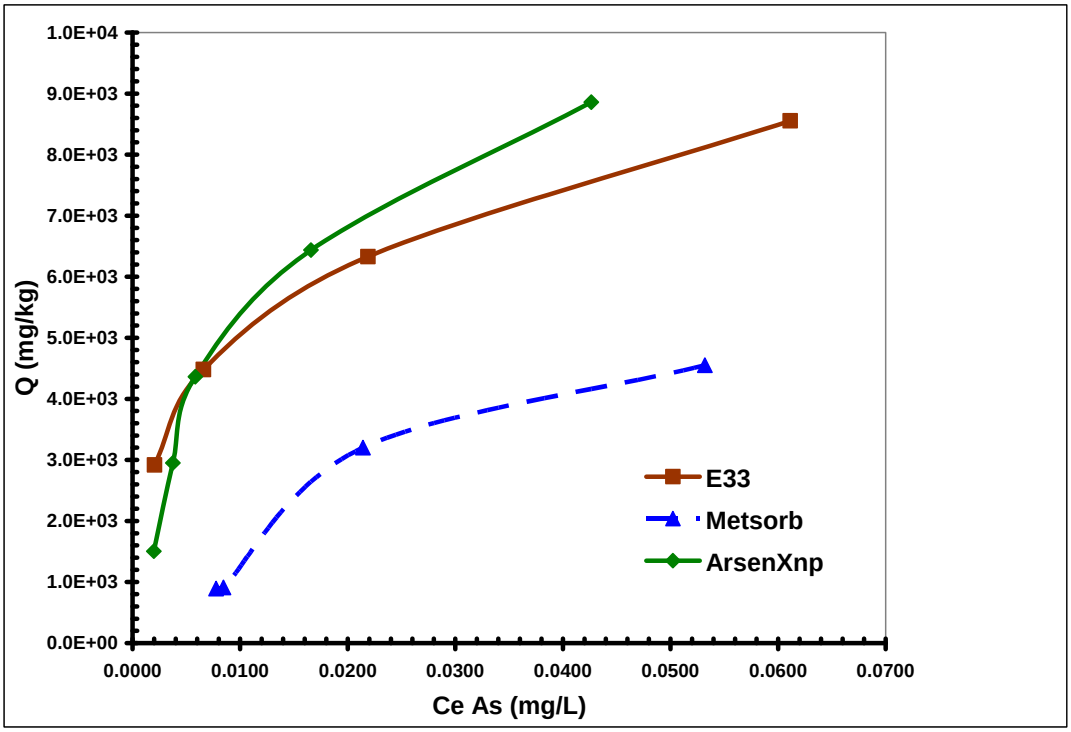

Figure 7. Sorption isotherm plots for E33, Metsorb and ArsenX^{np}

4.0 DYNAMIC STUDIES

4.1 Pilot Tests

Design

The design of the pilot system and intended standard operating procedures are described in detail in the Pilot Test Specific Test Plan (PTSTP) for the Socorro Springs Pilot (Siegel et al. 2006a). The pilot test skid contained ten columns, each designed as independent arsenic adsorption media filters operating in parallel. Each column is modular in design consisting of the following components: rotameter, three-way valve (for service or backwash mode), up-gradient pressure gauge, column with adsorptive media, down-gradient pressure gauge, another three-way valve (service or backwash mode), sample tap, totalizing flow meter, check valve, and all associated piping. During the pilot test, the flow rate, cumulative flow, pressure drop across the media and the corresponding backwash requirements (frequency and volume) were measured. The arsenic adsorptive columns were designed based on information on particle size, desired hydraulic loading rate, and optimum empty bed contact times (EBCTs) supplied by the vendors (Siegel et al. 2006a).

Table 7. Summary of Final Pilot Design

Vendor Media	MetSorb	E33			ArsenX^{np}
Number of Pilot Scale Columns	**1**	**3**			**1**
Hydraulic Loading Rate (HLR), gpm/ft^2	**8**	**6**			**8.2**
Column Number	SC-6	SC-8	SC-9	SC-10	SC-5
EBCT, minutes	2	2	4	5	3
Column Height, (Hc), inches	39	39	60	60	60
Column Diameter (D), inches	3	3	3	3	3
Media Depth (Hm), inches	25.7	19.3	38.5	48.1	39.2
Media Volume (V), liters	2.97	2.23	4.50	5.57	4.74
Water Flow rate (Q), gpm	0.4	0.3	0.3	0.3	0.4
Face Velocity (v), ft/min	1.07	0.80			1.09
Backwash Flow rate (Q_{BW}), gpm	0.3	0.3			0.2

The arsenic adsorption media filters operated continuously during the test with the exception of the potential for an occasional backwash (as required by unacceptable head loss across a filter bed). Water samples were taken daily for the first two weeks of the test and twice weekly for the remainder of the test. Field operation, maintenance procedures, sample collection and sample management are described in the PTSTP (Siegel et al, 2006a) and the Pilot Test report (Siegel et al, 2007.) At the conclusion of the test, pore water samples were taken at regular intervals from several of the columns. The media were removed from each column and returned to SNL for post-test characterization. Toxicity Characteristic Leaching Procedure TCLP (USEPA 1992) and California Wet Extraction Test CA WET (Sate of California 2005) analyses were performed for each media prior to final disposal.

Pilot Test Results

Breakthrough curves for arsenic in the pilot test columns are shown in Figures 8, 9 and 10. In Figure 8, the arsenic concentration in the chlorinated influent is compared to the arsenic concentrations for each sampling event. Note that changes in the arsenic concentration of the influent are often correlated with changes in the effluent. In some cases, concentration spikes in the effluent bring the arsenic levels in the effluent above the MCL for short periods of time. Figure 9 compares the arsenic concentrations at equivalent numbers of bed volumes of flow through the columns for three media run at the EBCT recommended by the vendor media through July 19, 2005.

Figures 8 through 10 show that arsenic (as As(V)) was removed completely from the chlorinated water initially in all of the columns and that as the capacity of the media for arsenic was exhausted over the course of several months, arsenic concentrations in the effluent rose. Figure

8 shows that the influent arsenic concentration was variable over the course of test period, ranging from 35 ppb to 55 ppb. This variability may result from non-uniform mixing of water from the two sources of water that feed the Socorro Springs well site. Detailed information including the breakthrough curves for other solutes, interlaboratory calibration studies, operational data, and results of TCLP and CA WET are found in Siegel et al. (2007). Figure 10 shows the breakthrough curves for the E33 run at three different EBCTs (2 min., 4 min. and 5 min.) The uncertainty in the method used to estimate the breakthrough point (visual examination of the curves) is estimated to be 15%. It is important to note that the EBCTs used in the tests were within the ranges recommended by the vendors and that the relative performance of the media could change if different EBCTs are used.

Table 8 summarizes the results of the pilot tests shown in Figures 8 through 10. The results of the tests are expressed as bed volumes of effluent that passed through the column until the effluent arsenic concentration reached 10 ppb It can be seen from inspection of Figures 9 and 10 that the number of BVs of influent, passing through the column until a target concentration is reached in the effluent, can be hard to estimate if the data are noisy. Thus, the number of BVs until breakthrough can be a very imprecise measure of the arsenic adsorption capacity of the media.

The estimates of the concentration of arsenic (mg As/g media) in the adsorptive media (i.e. the capacity) at effluent concentrations of 10 ppb (10 μg/L), when $C/C_o = 0.8$ and when $C_e = C_o$ (where the influent (C_o) and effluent (C_e) concentrations are equal) are also shown in the table. The capacities are calculated from mass balance on arsenic data by integration of the area above the breakthrough curves (BTC) and below the influent arsenic concentration. These may be a more unbiased measure of sorption than the BV value as discussed below. The capacity at 10 ppb (10 μg/L) is calculated from raw data from BV = 0 to the point in the BTC where the arsenic concentration in the effluent (C_e) reached and stayed above 10 ppb (10 μg/L). Lower limits for several of the parameters are listed in the table because the experiments were terminated before full or 80% capacity of the columns was reached. Other parameters in the table are discussed in later sections of this paper.

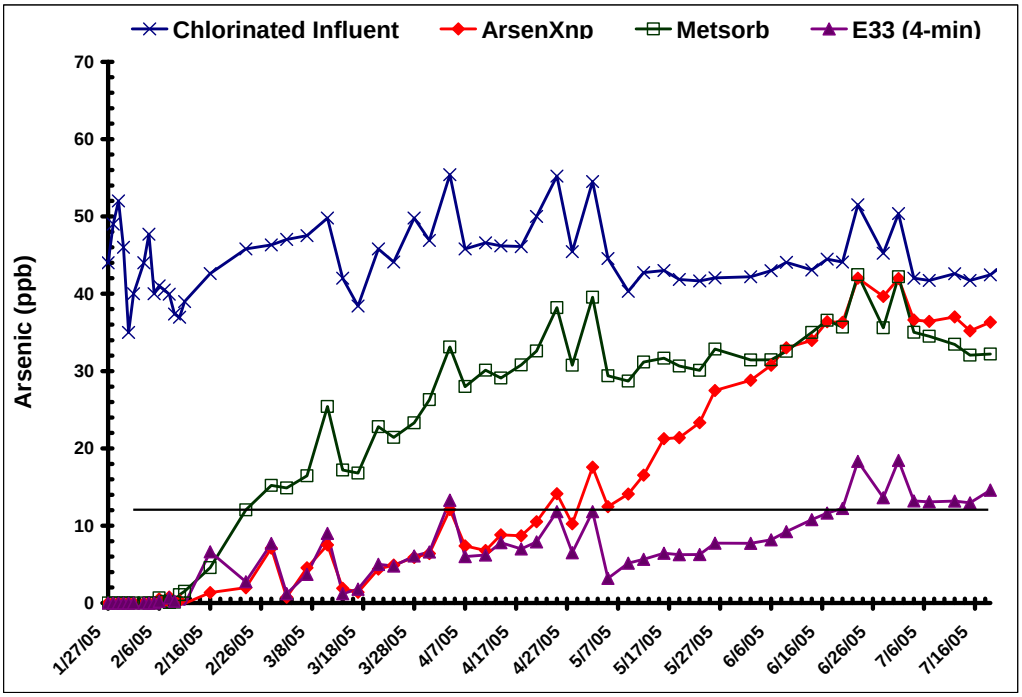

Figure 8. Arsenic Breakthrough and Influent Arsenic Concentrations for Adsorbent Media Columns at Socorro Springs.

Table 8. Summary of Performance Data for Adsorbent Media Using Three Methods.

		E33				Metsorb	ArsenX^{np}
		2 min	4 min	5 min			
Pilot	BV to 10 ppb (10 μg/L)	24,000	43,000	52,000		13,000	27,000
	Capacity at 10 ppb, mg/g	1.95	3.56	4.21		0.70	1.38
	Capacity at C/C_o = 0.8, mg/g	4.03	NA	NA		2.26	2.10
PD RSSCT	BV to 10 ppb (10 μg/L)	15,400	43,000	41,000		12,800	43,000
	Capacity at 10 ppb, mg/g	1.95	3.39	3.07		0.69	1.33
	Capacity at C/C_o = 0.8, mg/g	4.26	4.68	4.71		1.24	1.37
	Capacity at $C_e = C_o$, mg/g	5.08	5.61	5.02		1.31	1.38
Freundlich isotherm	Capacity at 10 ppb, mg/g	4.97				1.18	4.63
	Capacity at 40 ppb, mg/g	7.67				4.13	9.86

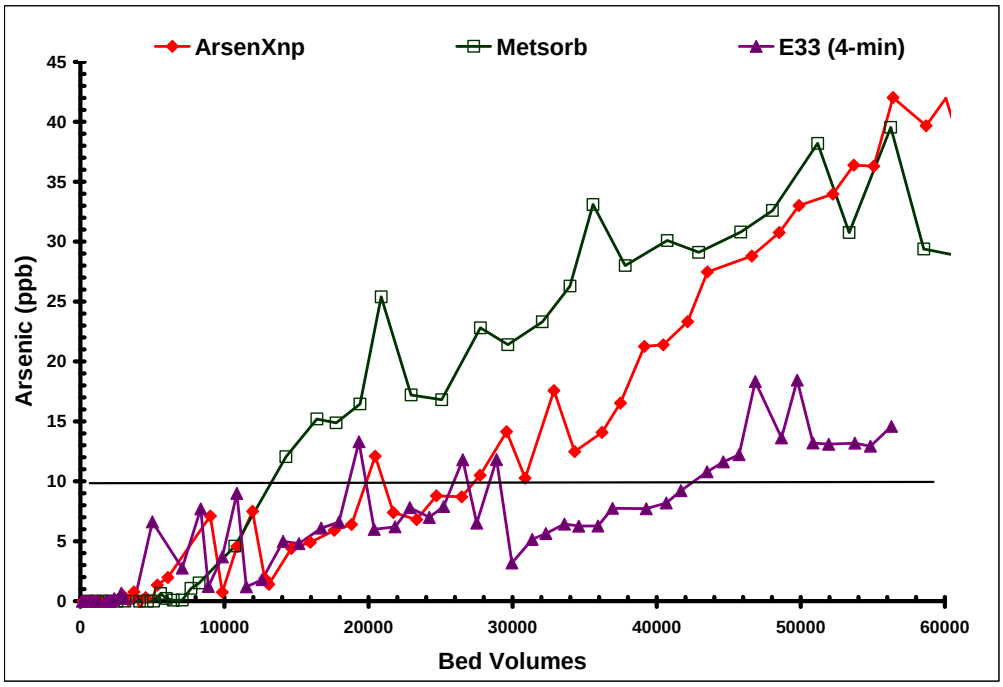

Figure 9. Arsenic Concentrations in Column Effluent as Function of Cumulative Bed Volumes.

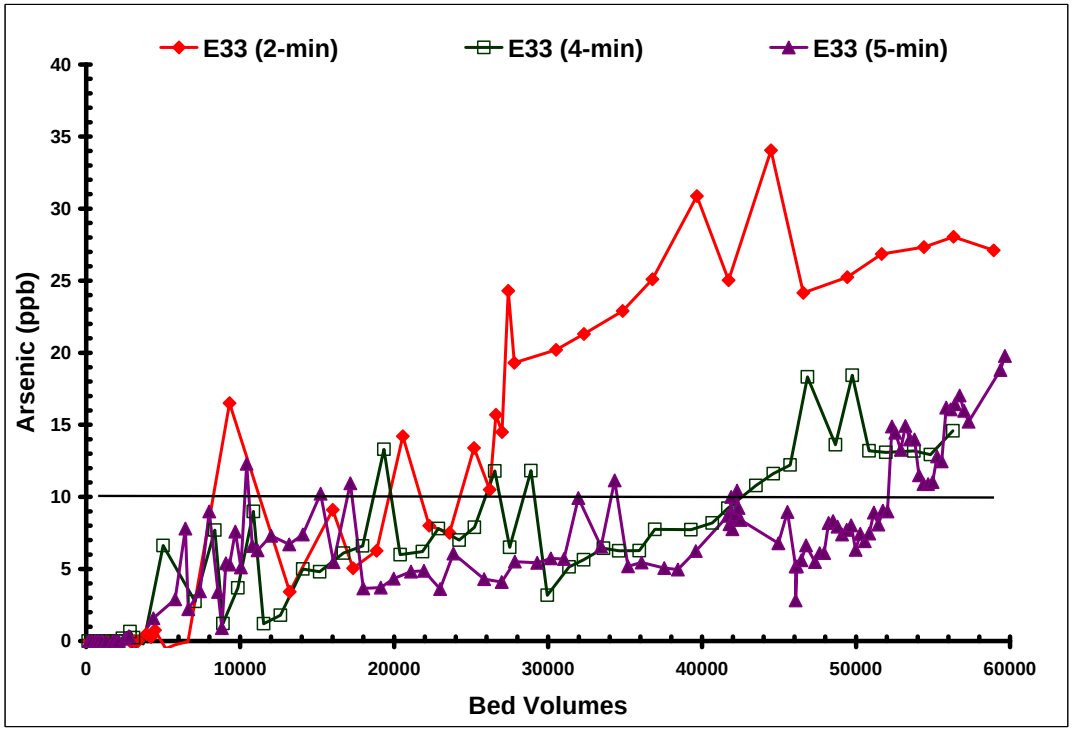

Figure 10. Arsenic Concentrations in Column Effluent as Function of Cumulative Bed Volumes for E33 with different EBCTs.

4.2 RSSCT Studies

Laboratory studies to predict media performance of pilot-scale adsorption columns were conducted using rapid small-scale column tests (RSSCTs). RSSCTs are scaled-down columns packed with smaller diameter adsorption media that receive higher hydraulic loading rates to significantly reduce the duration of experiments. (Aragon et al. 2004; Thomson et al. 2005; Westerhoff et al. 2005). Results for RSSCTs can be obtained in a matter of days to a few weeks, whereas pilot tests can take a number of months to over a year.

This method uses scaling relationships that allow correlation of lab-scale column results operated at accelerated flow rates to full-scale column performance. The RSSCT concept is based upon a theoretical analysis of the adsorption processes that govern performance including solution and surface mass transport and adsorption kinetics. Mass transfer models have been used to determine dimensionless parameters that establish similitude between the small- and large-scale columns. Crittenden et al. (1987a, 1987b, 1991) developed scaling equations for both constant and non-constant diffusivities with respect to particle size. The scaling laws ensure that the RSSCT and the full-scale system will have identical breakthrough profiles. Details of the theoretical basis for the RSSCT method are described in Appendix 2. Proportional diffusivity (PD) and constant diffusivity (CD) tests were carried out for the media studied in the Socorro Springs pilot test (Siegel et al. 2007). Design, procedures and results for the proportional diffusivity tests are described in detail in Aragon (2007) and are summarized below.

Methods and Materials

Media shipped from the vendors was crushed by hand or with a mechanized mortar and pestle (shatterbox), separated by sieve stack into mesh fractions, and rinsed with DI water to remove fines. The E33 and Metsorb were baked in oven at 105°C overnight to complete dryness. For column packing, dry media was weighed according to design calculations described in Appendix 2, submerged in DI water and deaerated by vacuum pump for at least one hour. The PD RSSCT columns were packed with 100x200 mesh adsorption media (diameters of 0.15 – 0.075 mm). Deaerated media was loaded into the columns as a slurry using a small spatula. Media was backwashed with DI water for approximately 15 minutes or until backwash water was clear of fines.

Chlorinated Socorro Springs water was hauled to SNL in 55 gallon drums for the RSSCTs and stored in 200 L feed tanks. Water was gravity fed to a manifold and to multiple columns, which were operated in down-flow mode. Pressures in the system did not exceed 20 psi. PD RSSCT column influent and effluent were sampled once per day via 3-way stopcock sample ports. Samples were filtered through 0.45 μm nylon membranes; approximately 50 mL of sample was collected and preserved with HNO_3 to achieve pH ~ 2. An internal standard and matrix spike (1-g 1250 ppb Ge and 1250 ppb As mixture) was added to each sample and analyzed for total arsenic with ICP-MS. Design parameters for RSSCTs and corresponding pilot scale test are shown in Table 9.

Table 9. Comparison of Design Parameters for Pilot-Scale and Small-Scale Columns

Parameter	Pilot Scale	RSSCT	Units
Column Diameter	7.6 (3)	1.0 (0.4)	cm (in)
Particle Diameter	0.25-2.0	0.15-0.18	mm
EBCT	2-5	0.05-0.9	min
Bed Height	50-130 (20-50)	8-30 (3-12)	cm (in)
Flow Rate	1,100-1,900 (0.3-0.5)	20-120 (0.005-0.03)	mL/min (gpm)
Hydraulic Loading Rate	24-32 (6-8)	15-125 (3-32)	cm/min (gpm/ft^2)

Actual EBCTs for the PD test columns were as follows: E33 – 0.23 min (PD 1-2); 0.38 min (PD 2-2); 0.50 min (PD 2-3); ArsenX^{np} – 0.28 min; Metsorb – 0.39 min

Results

Breakthrough curves for the E33 media at 3 EBCTs are shown in Figures 11a – 11c; curves for Metsorb and ArsenXnp are shown in Figures 12 and 13. RSSCT PD and Pilot test data are shown for comparison. The shapes of only the 2 min. and 4 min. EBCT E33 pilot tests correlate well with their corresponding RSSCTs. Results are summarized in Table 8 above; the RSSCTs are reasonably good predictors of the number of BVs to reach 10 ppb As for the E33-4 min EBCT and Metsorb pilots tests but less accurate for the other EBCTs for E33 and the ArsenX^{np} pilot tests. The estimates of the adsorptive capacity of the media, i.e. the concentration of arsenic (mg As/g media) at effluent breakthrough concentrations of 10 ppb (10 μg/L), at $C/C_o = 0.8$ and at $C_e = C_o$ (where the influent (C_o) and effluent (C_e) concentrations are equal) are also shown in Table 8. The capacities are calculated from mass balance on arsenic data by integration of the area above the BTC and below the influent arsenic concentration. As discussed previously, these may be a more unbiased measure of sorption than the BV value.

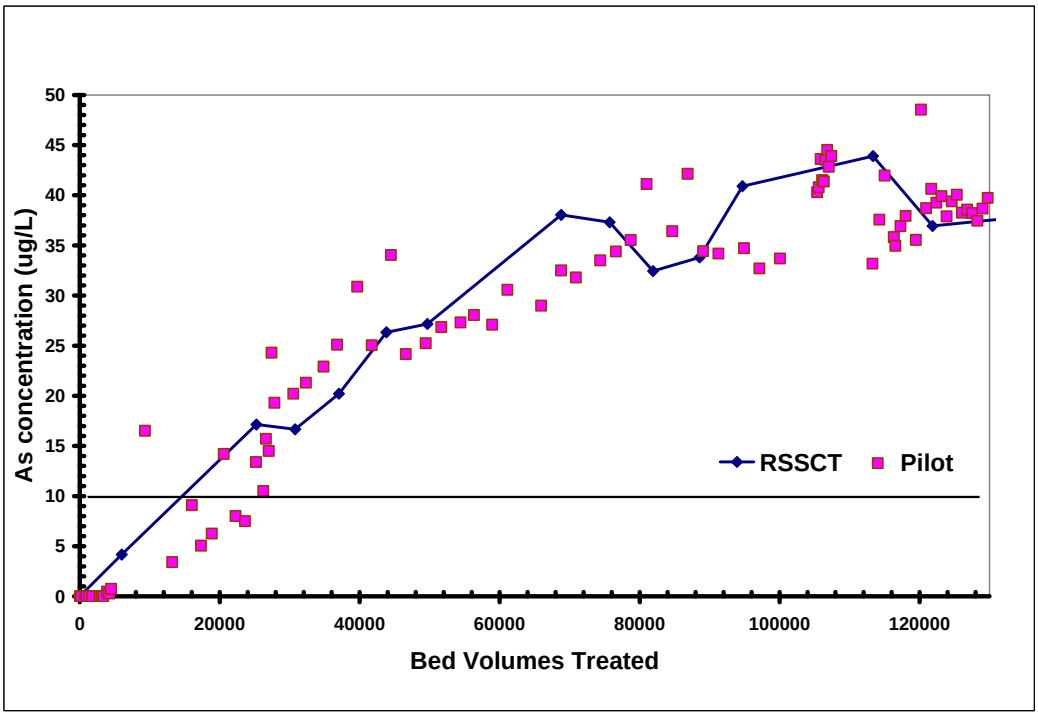

Figure 11a. Pilot and RSSCT (PD 1-2) Breakthrough Curves for E33 Media for 2 minute EBCT.

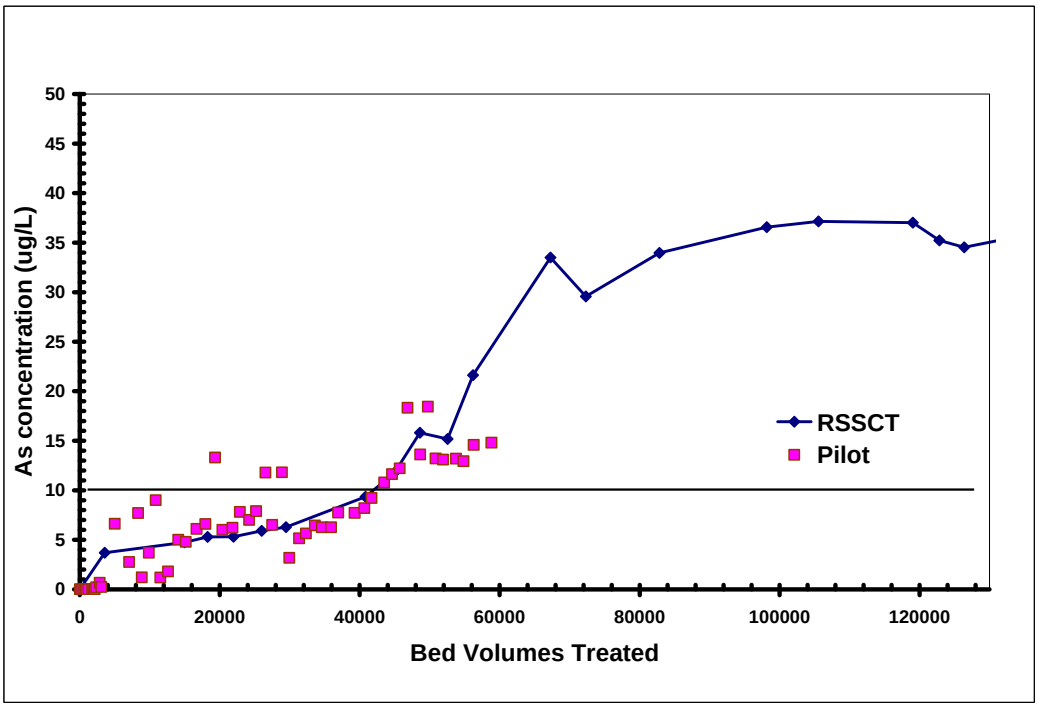

Figure 11b. Pilot and RSSCT (PD 2-2) Breakthrough Curves for E33 Media for 4 minute EBCT.

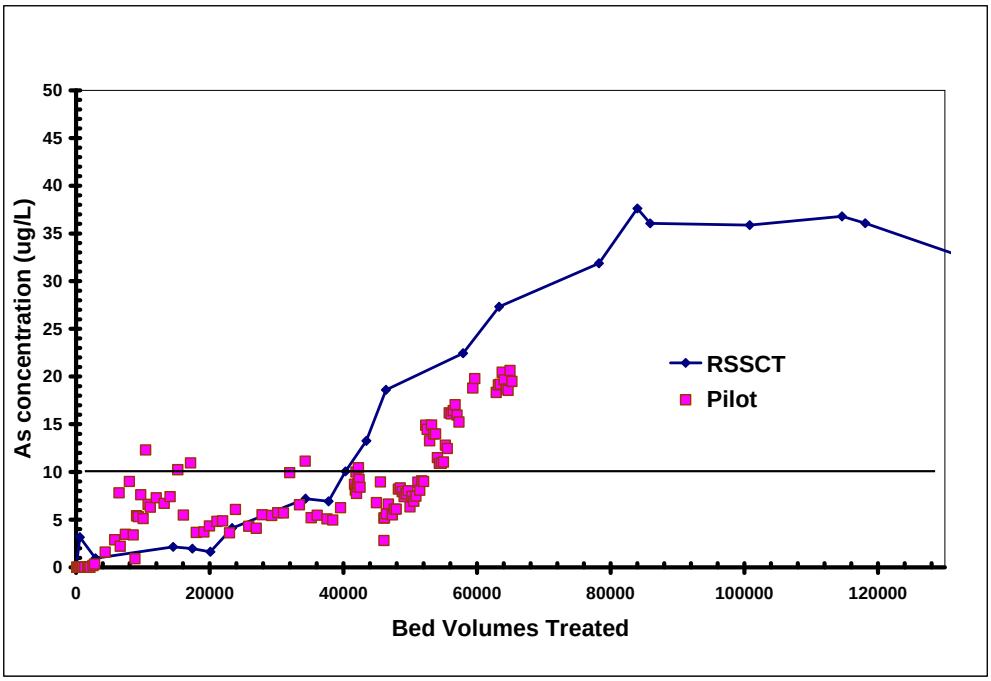

Figure 11c. Pilot and RSSCT (PD-2-3) Breakthrough Curves for E33 Media for 5 minute EBCT.

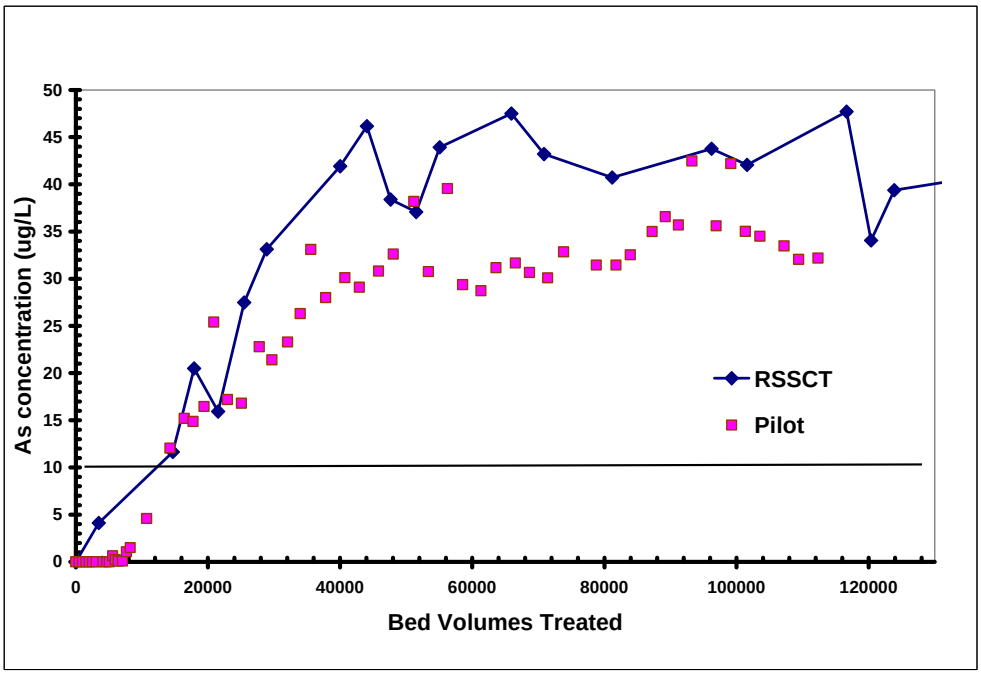

Figure 12. Pilot and RSSCT Breakthrough Curves for Metsorb Media.

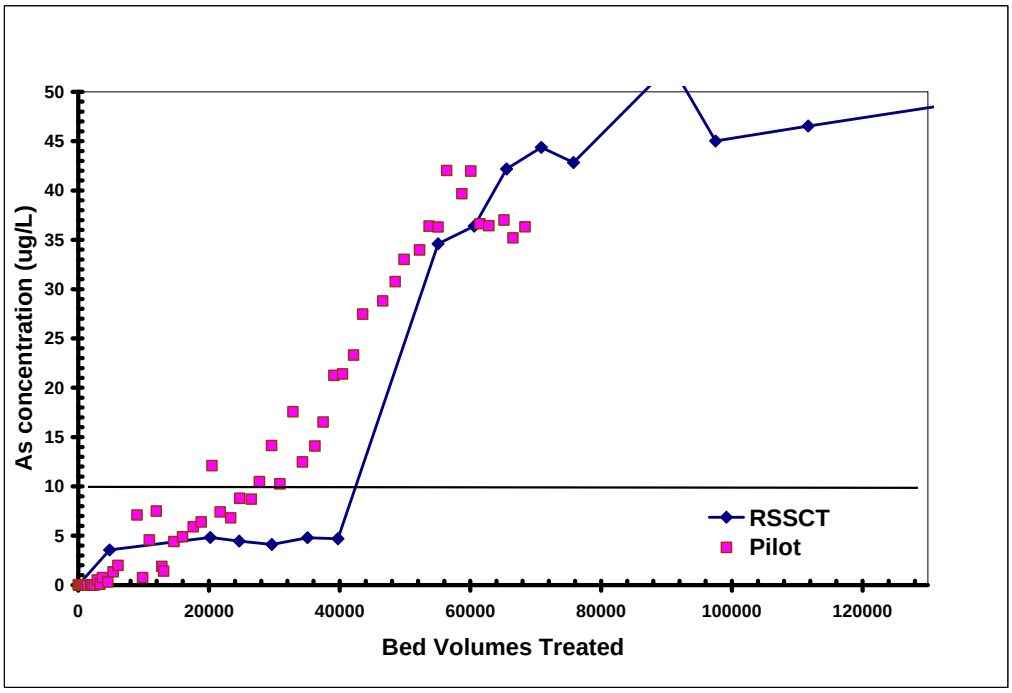

Figure 13. Pilot and RSSCT Breakthrough Curves for ArsenX^{np} Media.

5.0 DISCUSSION

5.1 Controls on Adsorption of Arsenic in Fixed Bed Media

To a first approximation, the effectiveness of fixed bed adsorptive media for arsenic removal depends on three kinds of factors:

1) The chemical nature of the adsorbent affecting its ability to form electrostatic or specific chemical bonds with arsenic oxyanions;
2) the physical properties of the media including surface area and pore size distribution of the adsorptive media, and any changes in hydraulic properties of the media during treatment, and
3) the chemistry of the water source including pH, redox speciation of As (i.e., As(III)/As(V) ratio), and the concentration of aqueous species that will interfere with adsorption of arsenic by competing for adsorption sites, modifying adsorptive media surface charge, or physically blocking access of arsenic to the interior of the particles or grains of adsorptive media;

This study addressed the first two factors by examining the arsenic sorption capacity of three different metal oxyhydroxide media exhibiting a range of chemical compositions and contrasting physical properties. Comparison of the results of this study to similar studies carried out in other water compositions will allow evaluation of the effect of the third factors and will be subject of future publications.

As water passes down through a filter vessel containing fixed bed media, the arsenic concentration declines within the media until it is no longer detectable. As the upper portion of the media becomes saturated, the treatment region (mass transfer zone) progresses downward until all adsorptive capacity is used and complete arsenic breakthrough occurs. When the capacity of the medium is completely exhausted, the arsenic concentrations in the untreated and treated water will be the same.

Figure 14 describes important dynamic processes involved in uptake of arsenic by adsorbent media. Note the concentration axes on the right side of the figure. The concentration of arsenic decreases from c_b in the bulk solution, to c_s at the fluid solid interface, to c_p in the pores, as q, the concentration in the solid, increases. In dynamic systems, such as fixed bed treatment systems, the effectiveness of arsenic adsorption is dependent on the relative rates of several processes. These include: 1) kinetics of surface complexation; 2) the rate of mass transfer of arsenic to the interior of the grains, and 3) the hydraulic loading rate (flow rate). The effectiveness of treatment will be highest when the arsenic species form specific chemical bonds quickly to reactive surfaces and the flow rate is low enough to allow arsenic species to migrate to fresh sorption sites in the grain interiors. High surface area and a uniform pore distribution with a mean pore size large enough to allow diffusion of the aqueous species lead to high sorption capacity.

The zero point of charge (ZPC) of the oxide is a property of the surface chemistry of the media and is an important determinant of adsorption capacity. Above the pH of the ZPC, the oxide surface has a net negative charge, and there will be an electrostatic repulsion between an anionic species and the surface. In this study, the arsenic adsorption capacities of media containing iron oxyhydroxide (E33, ArsenX^{np}), and titanium oxyhydroxides (Metsorb) were compared. Two iron oxyhydroxide phases were examined: E33 is composed of granules of a mixture of iron oxyhydroxide phase; in ArsenX^{np}, nanoparticulate iron oxide is dispersed within an ion exchange resin bead. In the alkaline, chlorinated water used in the Socorro Springs pilot study, arsenic is predominantly present as the oxyanion arsenate. The ZPC's of the oxide phases in the media are not well characterized, but in general, iron oxyhydroxide and the titanium oxyhydroxides have ZPC's about pH = 6.7 (Yoon et al. 1979). Thus, at the ambient pH, (about 8) both of the metal sorbents exhibit a negative surface charge. If sorption is to occur by a specific chemical bond, the electrical repulsion must be overcome in these media. Differences in adsorption capacity among the media in batch experiments are likely due to specific chemical adsorption and the physical properties of the media that affect arsenic diffusion into the interior of the grains.

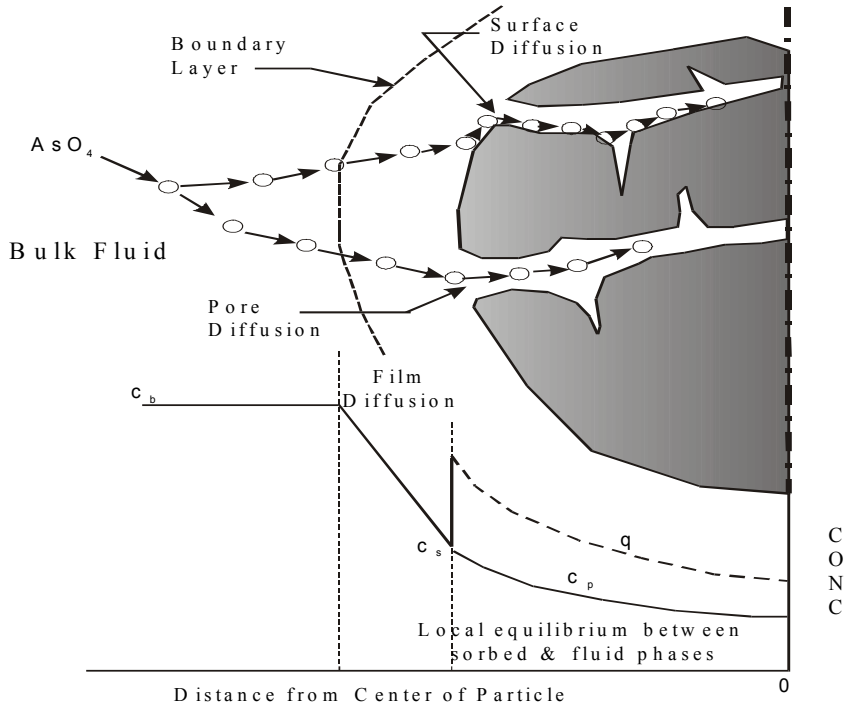

Figure 14. Processes Controlling Transport of Arsenic from Bulk Solution to Interior of Granular Adsorbent Media (adapted from Crittenden 1987b).

In a flowing system, the balance between the rates of the chemical and physical processes is expressed by the shape of the mass transfer zone (MTZ). In the MTZ, the concentration of the arsenic drops from its initially high value to a lower value corresponding to equilibrium sorption. The shape of the MTZ is very important to use of adsorptive media in drinking water treatment. The adsorbent bed must be replaced or regenerated when the concentration of arsenic in the effluent exceeds the MCL (10 µg/L). Under favorable conditions where diffusion into the grain interior is rapid relative to flow (hydraulic loading) rate, the mass transfer zone will be relatively sharp, and a large fraction of the potential sorption capacity of the media will be utilized before replacement is warranted. Under unfavorable conditions, the mass transfer zone will be broad, the arsenic concentrations in the effluent will rise rapidly above the MCL, and most of the adsorbent bed will not adsorb arsenic before it needs to be replaced. Prediction of the performance of adsorptive media in pilot tests or full-scale applications relies on information about the adsorptive capacity of the media in batch systems as well as the shape of the MTZ in the dynamic system. In the following section, the use of an analytical model to predict the shape of the MTZ is evaluated.

5.2 Modeling of Adsorption Breakthrough in a Packed Column – Klinkenberg Model

One of the goals of this project is to determine if the performance of adsorbent media in field scale tests can be predicted from relatively few laboratory measurements. A mathematical model that could be programmed in an excel spreadsheet was examined as a potential predictive tool. Details about the model are given in Appendix 3 and summarized below. This simple solution for an adsorption breakthrough curve is based on the following assumptions:

(1) Isothermal conditions;
(2) No axial dispersion;
(3) Linear driving force for mass transfer, i.e. constant k;
(4) Linear adsorption equilibrium, i.e. constant K (ρK_d).

If the overall mass transfer coefficient (k) and Henry's Law constant (K) are known, it is possible to predict:

1. the adsorption breakthrough curve at bed exit or any location inside the column {(c/c_f) vs. t}, and
2. the concentration profile inside the column {(c/c_f) vs. z} at any time (t).

There are two ways to determine the overall mass transfer coefficient k and Henry's Law constant K**:** (1) from batch experiments (adsorption equilibrium and kinetics) as described in the preceding sections and (2) from breakthrough data obtained in small or large columns by regression. The second approach is applied in this section by modeling the adsorption breakthrough curves of arsenic from the packed columns of E33 and Metsorb media used in the RSSCTs.

Equation (9) is an analytical solution (Klinkenberg 1948) of the ratio of adsorbate concentration in the fluid phase to that of influent at a given location (z) and a given moment (t).

$$\frac{c}{c_F} \approx \frac{1}{2}\left[1+\mathrm{erf}\left(\sqrt{\tau}-\sqrt{\xi}+\frac{1}{8\sqrt{\tau}}+\frac{1}{8\sqrt{\xi}}\right)\right] \qquad \text{(Eq. 9)}$$

where c_F is the influent adsorbate concentration, τ is the dimensionless time coordinate, and ξ is the dimensionless distance coordinate. These are defines by:

$$\xi = \frac{kKz}{u}\left(\frac{1-\varepsilon_b}{\varepsilon_b}\right) \qquad \text{(Eq. 10)}$$

$$\tau = k\left(t-\frac{z}{u}\right) \qquad \text{(Eq. 11)}$$

where *k* is the overall mass transfer coefficient (min^{-1}), K is the dimensionless Henry's law adsorption equilibrium constant, and time t

As discussed in Appendix 3, the Klinkenberg solution also provides an analytical solution of the ratio of adsorbent loading to the equilibrium adsorption amount at a given location (z) and a given moment (t); therefore, it is possible to predict the adsorbent loading inside the column {i.e ($\bar{q}$ vs. z} at any time.

Modeling of Adsorption Breakthrough of Arsenic from Packed Columns

RSSCT PD 2-2 data for E33, as shown in Table 10 were used as the basis for regressing the overall mass transfer coefficient k and Henry's Law constant K (ρK_d) used in equation (2) for prediction of arsenic adsorption breakthrough at other conditions. The EBCT of this RSSCTs corresponded to the 4 minute EBCT of the pilot tests for E33. It was assumed the bed porosity ε_b was 0.5 for all cases. Equations (2) to (4) were programmed into an Excel spreadsheet by fitting the experimental breakthrough data with equation (2), and the corresponding set of model parameter (k, K) for the column given in Table 10. As shown in Figure 15, the Klinkenberg model fits the adsorption breakthrough curve for PD 2-2 quite well.

Table 10. RSSCT Parameters for Klinkenberg Model Calibration

Column Name	PD 2-2	PD 2-3	N/A	
Media Type	E33 - Medium EBCT	E33 – long EBCT	Metsorb	
Mesh Size	100x200	100x200	100x 200	
Column diameter	0.70	0.70	0.70	cm
Bed height	9.37	12.38	12.78	cm
Bed volume	3.61	4.76	4.92	cm^3=mL
Flow rate	9.50	9.50	12.70	mL/min
EBCT	0.38	0.50	0.39	min
Mass media	1.90	2.40	4.00	g
Average c_F	42.5	40.28	44.0	ppb

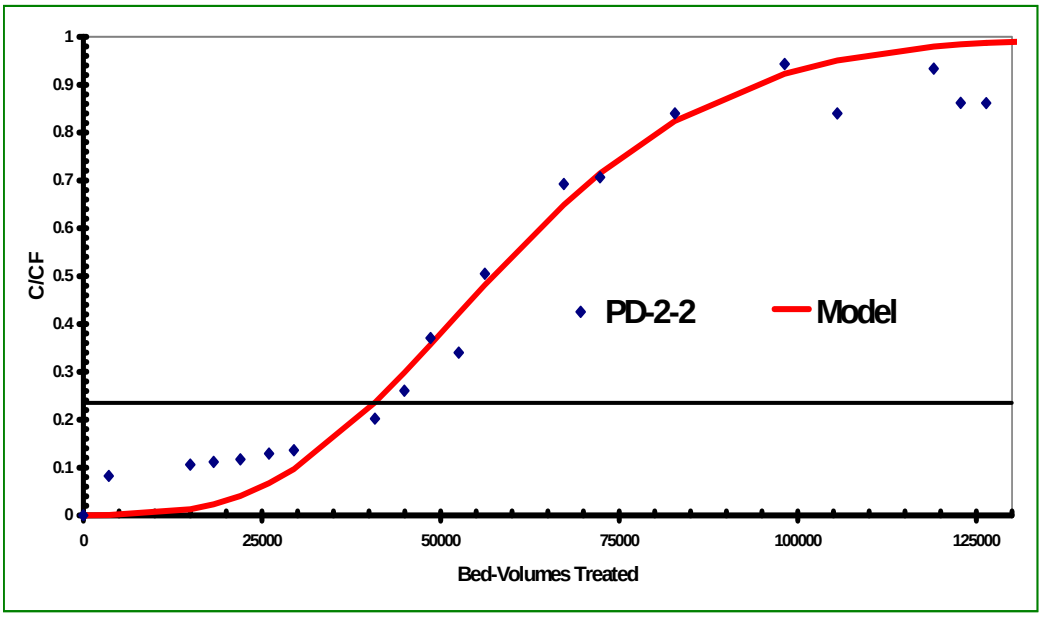

Figure 15. Calibration of As Breakthrough Data (PD-2-2) with Klinkenberg Model; k (min^{-1}) = 0.0005; K = 120,000.

Using the Klinkenberg model constants (k, K) determined from the RSSCT data, we should be able to predict the arsenic breakthrough performance of similar adsorbents at different operating conditions. Figure 16 shows that the Klinkenberg model with the model parameters (k, K) regressed from RSSCT data PD-2-2 (small particles, medium EBCT) can predict fairly well the breakthrough curves obtained from RSSCT PD-2-3, which has a longer EBCT. This suggests that breakthrough data obtained from a short column with a smaller empty-bed-contact-time (EBCT) can be used to predict the performance in a long column with a larger EBCT. This statement, if validated with other adsorbent media, could significantly reduce the number of RSSCT experiments required to evaluate alternative adsorbent media.

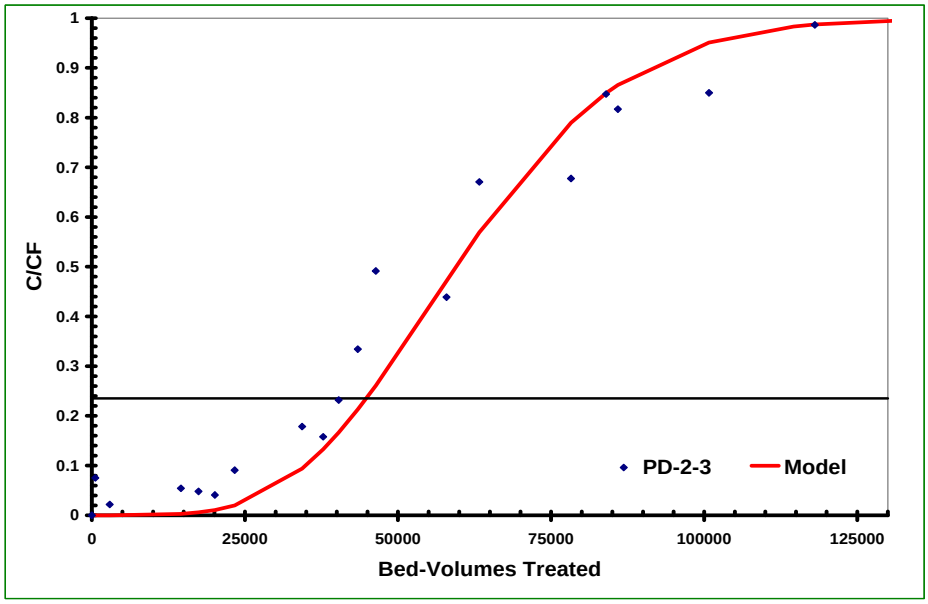

Figure 16. Comparison between Breakthrough Curves Obtained in RSSCT PD 2-3 with Predictions from Klinkenberg Model Using Parameters from RSSCT PD- 2-2.

Comparisons of breakthrough curves obtained from pilots test SC-8, SC-9 and SC-10 to the predictions from the Klinkenberg model using the model parameters (k, K) regressed from RSSCT data PD- PD-2-2 are shown in Figures 17 to 19. These are scale-ups from the small RSSCT column to a much larger column (scale-up ratio of 2600 times). The pilot test conditions are summarized in Table 7.

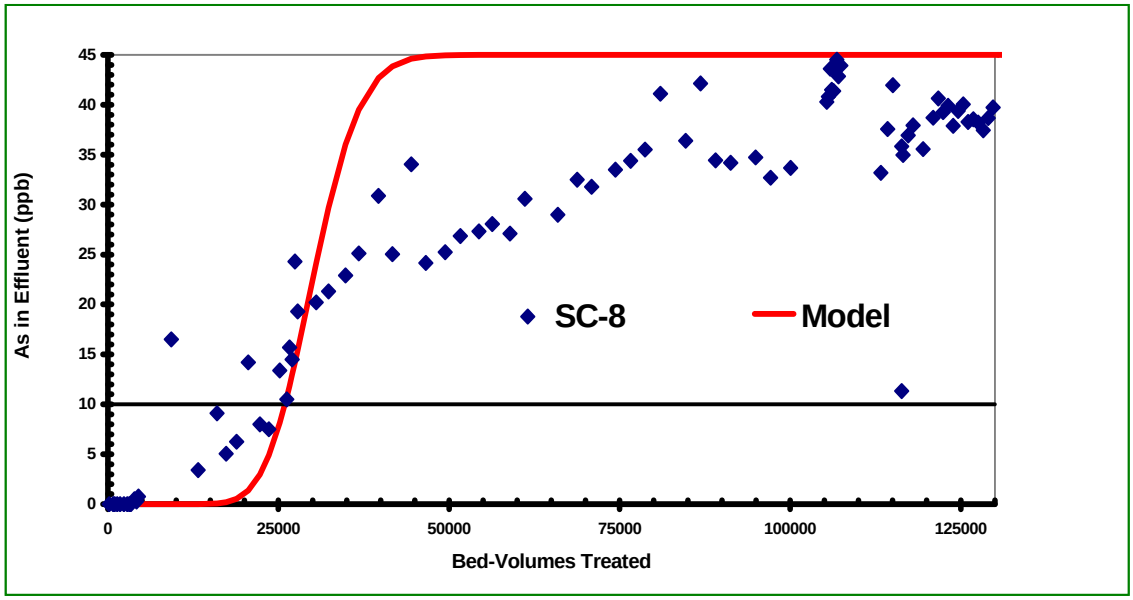

Figure 17. Comparison between Breakthrough Curves Obtained in Pilot Test Run SC-8 with Predictions from Klinkenberg Model using parameters from RSSCT PD- 2-2. k (min^{-1}) = 0.0005; K = 120,000.

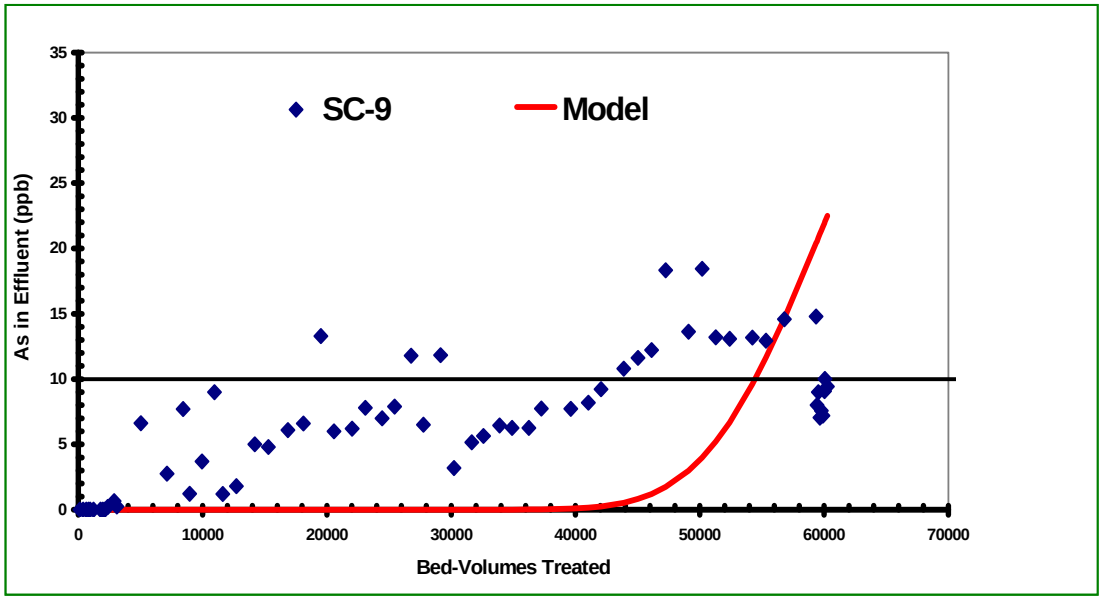

Figure 18. Comparison between Breakthrough Curves Obtained in Pilot Test Run SC-9 with Predictions from Klinkenberg Model using parameters from RSSCT PD- 2-2.

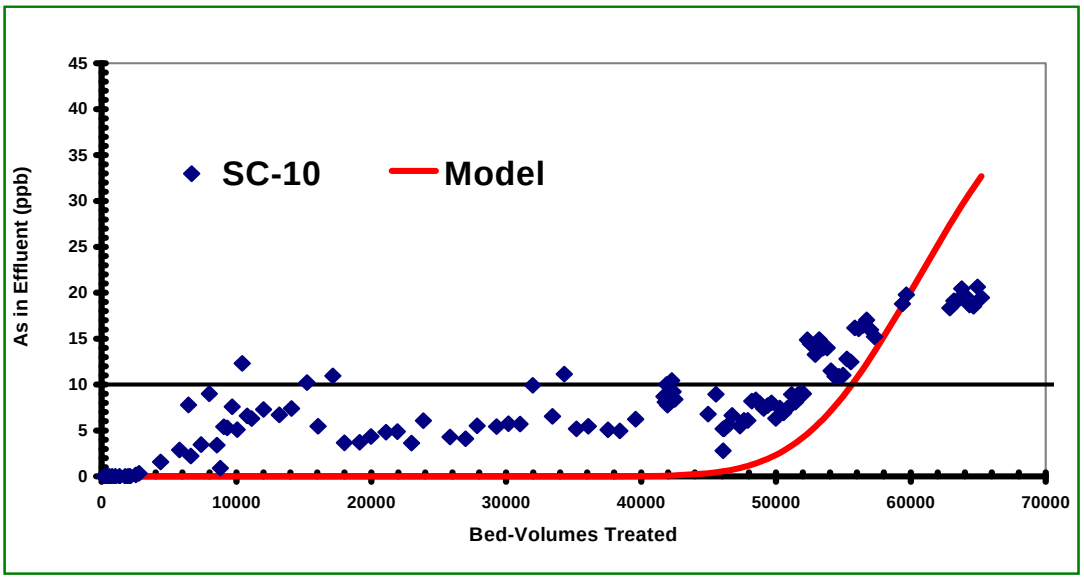

Figure 19. Comparison between Experimental Breakthrough Curves Obtained in Pilot Test SC-10 with Predictions from Klinkenberg Model using parameters from RSSCT PD- 2-2.

Although the shape of the breakthrough curve in the SC-8 pilot (2 min EBCT) disagrees with that of the model, both show 10 ppb breakthrough at about 27,000 BVs. The model predicts

breakthrough in SC-9 at 54,000 BVs compared to the 42,000 BV estimated from the pilot test data. The model prediction using RSCCT data PD-2-2 for the SC-10 pilot (5 min EBCT) agrees well with the experimental breakthrough curve and forecasts similar value of breakthrough time as the experimental data (~55,000 BVs vs 52,000 BV). Because there is so much scatter in the pilot test data, any comparison to the exact BV value predicted by the analytical model should be considered semi-quantitative at best.

Figure 20 compares the pore water arsenic concentration profile inside column SC-10 and the predicted arsenic concentration profile from the Klinkenberg model using the values of k and K regressed from RSSCT data PD-2-2. It is interesting to note that the model can semi-quantitatively predict the shape of the pore water arsenic concentration profile inside the column. Theoretically speaking, the adsorption breakthrough curve at the column exit and the concentration profile inside the column at the breakthrough time are symmetrical. This information can be utilized to design accelerated pilot scale tests to replaced prolonged breakthrough experiments. Instead of measuring the breakthrough at the column exit for an extended period of time, it may be possible to measure the concentration profile inside the bed once the steady state is established. By analyzing the concentration profile, one can obtain a set of model parameters (k, K) and apply these parameters to predict the adsorption breakthrough at the column exit.

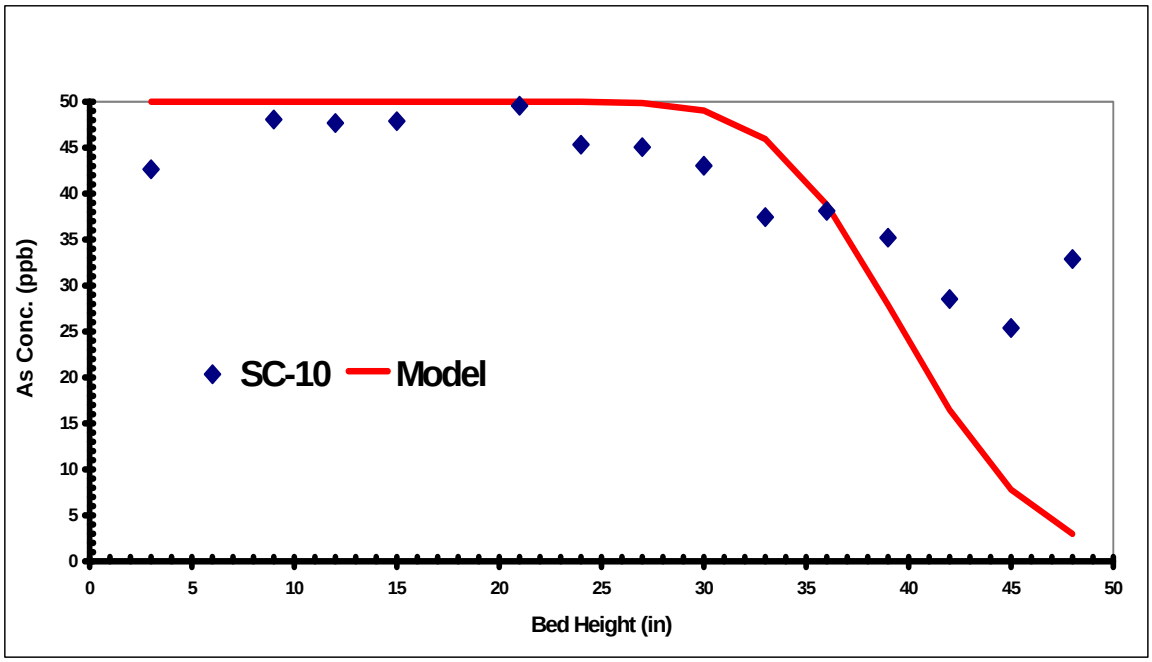

Figure 20. Pore Water Comparison between Experimental As Concentration Profile Obtained in Pilot Test Run SC-10 with Prediction from Klinkenberg Model PD-2-2 (k=0.0005 min^{-1}, K=120,000).

Data from the Metsorb RSSCT column (Fig. 12) were also regressed with the Klinkenberg model to obtain values of k (0.004 min-1) and K (50,000). Figure 20 compares pilot scale data to predictions made with the Klinkenberg model using these parameters (solid line). The model

gives a reasonable estimate of the BV at 10 ppb breakthrough but does not match the rest of the curve. Using a value of K consistent with the best linear fit to the sorption isotherm (K (ρK_d) = 95,000; see Table 6) does not improve the fit (curve marked pilot fit K=95K). Decreasing the mass transfer coefficient to k = 0.000065 improved the fit considerably (curve marked best Pilot fit K). This suggests that the model could be used with batch sorption data in sensitivity analyses to semi-quantitatively predict both the breakthrough at the MCL and the shape of the elution curve if independent information about the mass transfer coefficients was available.

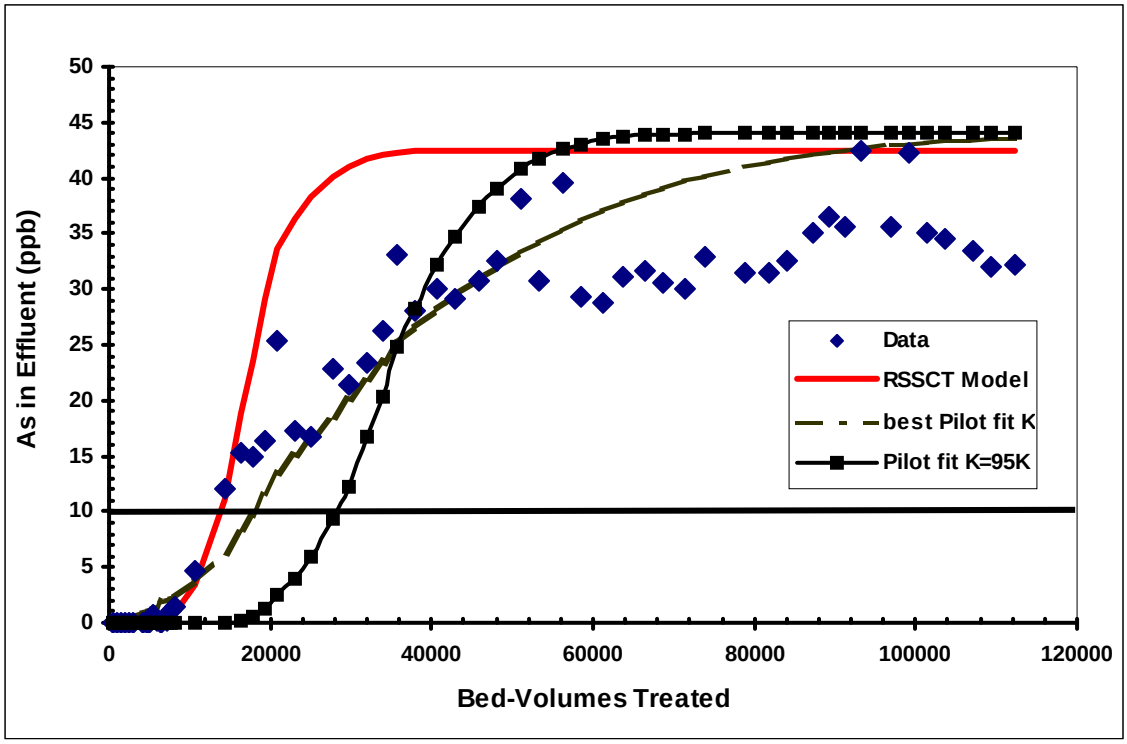

Figure 21. Comparisons among Breakthrough Curves Obtained in Metsorb Pilot Test with Predictions from Klinkenberg Model using Parameters from RSSCT and Alternative Model Fits. RSSCT: k = 0.0004, K = 50,000; Pilot test K= 95K: k = 0.0004; K = 95,000; best Pilot fit K; k = 0.000065; K = 95,000.

The results also suggest that the Klinkenberg equation might be used to estimate the pilot test breakthrough at the MCL for different EBCTs using data from a single RSSCT. Such an application could limit the number of RSSCTs needed to accurately predict breakthrough for full-scale systems of different sizes and costs. In this study, the pilot breakthrough for the three EBCTs is estimated by the model predictions derived from the RSSCT curves run at the intermediate EBCT.

5.3 Comparison of Estimates of Media Performance Using Batch and Dynamic Tests

In this study, four experimental methods were used to estimate the likely performance of adsorbent media in a full-scale treatment system at Socorro Springs: two batch sorption measurements (kinetic and equilibrium), RSSCTs and a pilot scale test. Results from all methods are summarized in Tables 8 above and in Table 11 below. In Table 11, the capacities predicted by the batch tests and RSSCTs are compared to those measured in the pilot tests. The relative number of bed volumes until breakthrough at 10 ppb predicted by the RSSCT agreed with that of the pilot test (E33 > ArsenX^{np} > Metsorb.) The relative adsorptive capacity (mg As/g media) at 10 ppb breakthrough for the pilot test, RSSCT and sorption isotherm measurements also followed the same order. Note that the capacities obtained in the isotherm tests are higher than those estimated from the pilot tests. (Table 8). This is consistent with the expectation that the smaller particle sizes and longer contact times in the batch tests would lead to more effective mass transfer of arsenic into the interior of the adsorptive media grains.

The level of absolute agreement between different laboratory test and pilot test performance was media-dependent. The number of bed volumes until breakthrough at 10 ppb measured by the RSSCTs for E33 and Metsorb were nearly identical to the values from the pilot tests, whereas the breakthrough in the RSSCT for ArsenX^{np} occurred at 63% of the volume in the pilot test. The sorption capacity (mg As/g media) of two of the media (E33, Metsorb) as measured in the pilot tests could be predicted to within about 70% by batch sorption tests, whereas the capacity of the ArsenX^{np} measured in the batch was much higher (336%) than that measured in the pilot test. The PD RSSCTs were accurate predictors of the media capacity for the pilot tests for E33, Metsorb and ArsenX^{np} media (within 5%) (Table 11).

The poor correlation between isotherm studies and column (RSSCT and pilot) predictions of arsenic removal by ArsenX^{np} is likely due to the behavior during crushing for the batch sorption and RSSCTs. The resin was ground to 325x400 mesh for isotherm studies. Upon crushing, the near perfectly spherical AsX^{np} beads were ground into what looked like a fine iron powder. Visually, the media did not seem have the same physical properties as the pre-crushed resin. Prior to crushing, the beads were comparable to ball bearings; after crushing, the media no longer seemed to be in a bead-like form. The fine materials were flakes that produced a red stain on contact. The sorptive properties of the ArsenX^{np} in the isotherm tests are probably not indicative of the performance to be expected in column or pilot studies. The properties of this material dominated the results of the batch sorption experiments and to some extent the RSSCT and make comparisons with the other media questionable. In addition to the effects of crushing on adsorptive properties, it was observed that the hydraulic properties before crushing were more ideal; water flowed through almost without resistance. After crushing, the media tended to stick together causing columns to ‘plug’ when water pressure was applied.

The ArsenX^{np} resin beads, however, were used in the kinetic batch tests and the pilot studies without crushing. These studies likely provide more accurate estimates of capacity and performance.

Table 11. Estimated Sorption Capacities from Lab Tests Relative* to Pilot Test Results.

Test	Media		
	E33 (4 min)	Metsorb	ArsenX^{np}
RSSCT-PD	0.95	0.99	0.96
Freundlich	1.40	1.69	3.36

* calculated as [capacity in As mg/g media]$_{test}$/[capacity in As mg/g media]$_{pilot}$

The Klinkenberg model can be used to calculate the breakthrough curves using values of the mass transfer coefficient (k min.$^{-1}$) and Henry's constant (dimensionless K_d or (ρK_d)). When values for theses variables are obtained from RSSCT experiments, the number of bed volumes of water treated until the MCL is reached could be predicted within 20% for the E33 media at three EBCTs and for the Metsorb media, however, the shape of the curves did not match the predictions. The inability of the model to match the pilot scale data may be due to the model assumption of linear sorption and to the dependence of the mass transfer coefficient on particle size. The first limitation is supported by the results of the batch sorption experiments; none of the media exhibited linear sorption (Table 6). The second limitation is supported by the results of other RSSCT experiments that showed a strong dependence on particle size for these and other media (A. Aragon, personal communication; Aragon, 2004). This suggests that a more accurate model of the adsorption breakthrough behavior would be possible with a non-linear adsorption isotherm and multiple pore diffusion resistances. The adsorption equilibrium and kinetic mass transfer data could be obtained from the batch adsorption experiment and RSSCT adsorption breakthrough data for this modeling effort.

6.0 SUMMARY AND CONCLUSIONS

Inexpensive, rapid tests are needed to predict the arsenic adsorption capacity of adsorptive media to help communities select the most appropriate technology for meeting compliance with the new arsenic MCL. In this study the consistency among capacity estimates made by batch and dynamic methods were compared and their relevance to full scale performance was evaluated. Each of the methods has inherent limitations and strengths. Pilot tests and RSSCTs provide direct estimates of the volume of water that can be treated in the column or adsorbent bed before arsenic in the effluent exceeds the MCL or other desired concentrations. However, the RSSCTs can only performed by highly trained specialists and the pilot tests are relatively expensive and take long times to obtained direct measurements of the treatment capacity. The results of both these tests may be subject to physical effects such as channeling and provide little direct information about plant operations. Batch sorption measurements are relatively rapid and inexpensive; they provide information about the equilibrium sorption capacity and kinetics of uptake of arsenic by relatively small particles. However, the results are not accurate indicators of the long-term performance of the media in full-scale treatment systems because they do not provide direct measurement of the shape of the mass transfer zone within an absorbent media column. In addition, they do not capture the effects of changes in the influent arsenic concentration on capacity.

The Sandia National Laboratories pilot demonstration at the Socorro Springs site obtained arsenic removal performance data for five different adsorptive media under constant ambient flow conditions; results for three of the media are reported here. Two iron oxyhydroxide phases were examined: E33 is composed of granules of a mixture of iron oxyhydroxide phase, in $ArsenX^{np}$, nanoparticulate iron oxide is dispersed within an ion exchange resin. The third media Metsorb, is a granular titanium oxyhydroxide. Test water was taken from blended well water at Socorro Springs. The water has approximately 45 ppb arsenic in the oxidized (arsenate – As(V)) redox state with moderate amounts of silica, low concentrations of iron and manganese and a slightly alkaline pH (about 8).

The amount of arsenic sorption by the media was studied using different methods to allow a clearer comparison of the relative performance. For the flow experiments (pilot and RSSCTs), a measurement was made of the number of BVs of water passing through the media columns until the regulatory limit (10 ppb [10 μg/L]) in the effluent was exceeded. For both the batch tests and the flow experiments, the sorption capacity of the media (amount of arsenic adsorbed by the media) when the treated water reached 10 ppb (10 μg/L) was also calculated or measured. For flow experiments, the capacities were calculated from mass balance on arsenic data by integration of the area above the BTC and below the influent arsenic concentration; these may be a more unbiased measure of sorption than the BV value. For batch tests, a sorption isotherm was fit to the data, and a capacity was calculated at 10 ppb (10 μg/L) or other values. In general, in the batch sorption studies, the media were ground to a smaller particle size than that used in the pilot test in order to minimize the effects of mass transfer within the grains and thereby reduce the time required to reach steady state. The batch equilibration time of 24 hrs was based on kinetic studies. Freundlich isotherms could be fit to sorption data from all of the media.

For the pilot tests using the EBCTs recommended by the vendors, the values of BV and capacity at 10 ppb (10 μg/L) arsenic show a fairly consistent relationship among the adsorptive power of the media:

$$E33 > ArsenX^{np} > Metsorb$$

For the Freundlich isotherm, the order of calculated sorption capacity in equilibrium with a solution with 10 ppb arsenic was: E33 > $ArsenX^{np}$ > Metsorb. Because the batch studies were designed to minimize kinetic and mass transfer rate effects, they provided upper limits to the arsenic adsorption capacity of the media. The calculated capacities in the Freundlich isotherms at 10 ppb (10 μg/L) were 1.4 times to 3.4 times the values measured n the pilot tests.

Rapid Small-Scale Column Tests are scaled-down columns packed with smaller diameter adsorption media that receive higher hydraulic loading rates to significantly reduce the duration of experiments. The PD RSSCTs were accurate predictors of the media capacity for the pilot tests for E33, Metsorb and $ArsenX^{np}$ media (within 5%)

The Klinkenberg analytical solution to the mass transfer equation of arsenic adsorption in a packed column can reasonably describe the adsorption breakthrough behavior of arsenic in E33 and Metsorb. Only two adjustable parameters: overall mass transfer coefficient k and Henry's constant K, are needed in this model for predicting adsorption breakthrough curve, adsorbate

concentration profile inside the column and adsorbent loading inside the column. The results suggest that the Klinkenberg equation calibrated on a single RSSCT might be used to provide reasonable estimates of pilot scale performance for a range of EBCTs . In this study the predicted breakthrough time is within 20% error of the experimental values obtained in the pilot tests. The model also was able to qualitatively predict the shape the mass transfer zone by calculating the arsenic concentration profile in the pore fluids of spent core from pilot test SC-10.

Laboratory tests (batch sorption and RSSCTs) are much less expensive to conduct than pilot tests and provide reasonable qualitative predictions of field scale performance. The results of this project suggest that laboratory studies could be useful to communities that cannot afford to carry out comparative pilot tests of multiple media, especially if other information about backwash requirements and costs (capital and labor) are already available. The goal of future work is to combine sorption data obtained at another site (Anthony) with the mass transfer coefficient obtained from Klinkenberg model from the Socorro study to see if breakthrough profiles can be predicted at the second site. Effort will also be devoted to model the adsorption breakthrough behavior with a non-linear adsorption isotherm and multiple pore diffusion resistances.

REFERENCES

Aragon, A. *Evaluation of Arsenic Adsorption Media*, 2004, thesis presented to the University of New Mexico, in Albuquerque, New Mexico, in partial fulfillment of the degree of Doctor of Philosophy.

Aragon, A. 2007, *Test Plan: Rapid Small Scale Column Tests (RSSCT) of Adsorptive Media for Arsenic Removal in Support of the Socorro, NM Pilot Demonstration Project*, Sandia National Laboratories, Albuquerque, NM.

Barrett, E. P., Joyner, L. G. and P. P. Halenda, 1951, The determination of pore volume and area distributions in porous substances. I. Computations from nitrogen isotherms*: J. Am. Chem. Soc.*, **73**: 373-380.

Berrigan, J. K., 1985*, Scale-up of rapid small-scale adsorption tests to field-scale adsorbers: theoretical and experimental basis*: Department of Chemical Engineering, Michigan Technological University, Houghton, MI**,** 202.

Crank J. *The Mathematics of Diffusion*, 2nd edition, 1976, Oxford Science Publications, New York, NY.

Crittenden, J. C., J. K. Berrigan, et al., 1987a, Design of rapid small-scale adsorption tests for a constant diffusivity: *Journal WPCF***, 58**(4): 312-319.

Crittenden, J. C., J. K. Berrigan, et al., 1987b, Design of rapid fixed-bed adsorption tests for nonconstant diffusivities: *Journal of Environmental Engineering:* **113**(2): 243-259.

Crittenden, J. C., P. S. Reddy, et al., 1991, Predicting gac performance with rapid small-scale column tests: *Journal AWWA*: **83**(1): 77-87.

Dixit, S. and J.G. Hering, 2003, Comparison of arsenic(V) and arsenic(III) sorption onto iron oxide minerals: implications for arsenic mobility. *Environmental Science and Technology*: **37**, 4182-4189.

Ford, R.G., 2002, Rates of hydrous ferric oxide crystallization and the influence on coprecipitated arsenate. *Environmental Science and Technology:* **36**, 2459-2463.

Hand, D. W. J. C. Crittenden, and W.E. Thacker, 1983, User-oriented batch reactor solutions to the homogeneous surface diffusion model. *Journal of Environmental Engineering Division*, Proceedings of ASCE, **109**(EE1): 82-101.

Hiester, N.K.; Vermenlen, T., 1952, Saturation performance of ion-exchange and adsorption columns, *Chem. Eng. Progress*, **48**, 505-516.

Ho, Y. S.and G. McKay, 1998**,** A comparison of chemisorption kinetic models applied to pollutant removal on various sorbents. Process Safety and Environmental Protection. *Process Safety and Environmental Protection:* **76B**, 332-340.

Ho, Y. S.and G. McKay, 2000, The kinetics of sorption of divalent metal ions onto sphagnum moss flat. *Water Res.:* **34**, 735-742.

Klinkenberg, A., 1948, Numerical evaluation of equation describing transient heat and mass transfer in packed bed, *Ind. Eng. Chem.* **40**, 1992-1994.

Lin, Z and R.W. Puls, 2000, Adsorption, desorption and oxidation of arsenic affected by clay minerals and aging process. *Environmental Geology:* **39** (7), 753-759.

Martinez, C.E., Jacobson, A., and M.B. McBride, 2001, Thermally induced changes in metal solubility of contaminated soils is linked to mineral recrystallization and organic matter transformations. *Environmental Science and Technology*; **35**(5), 908-916.

Meng, X.G., G.P. Korfiatis, C.Y. Jing, and C. Christodoulatos, 2001, Redox transformations of arsenic and iron in water treatment sludge during aging and TCLP extraction. *Environmental Science and Technology*; **35**, no.17, p.3476-3481.

North, K. P., 2006, *Attrition Loss Analysis for Arsenic-Removing Media*, SAND2006-0374, Sandia National Laboratories, Albuquerque, NM.

O'Reilly, S.E., D.G. Strawn, and D.L. Sparks, 2001, Residence time effects on arsenate adsorption/desorption mechanisms on goethite. *Soil Science Society of America Journal*; **65**, no.1, p.67-77.

Reddad, Z., C. Gerente, Y., Andres, and P. Le Cloirec, 2002, Modeling of single and competitive metal adsorption onto a natural polysaccharide, *Environ. Sci. Technol.* 36, 2067-2073.

Ruthven, D. M. *Principles of Adsorption and Adsorption Processes*, Wiley-Interscience, New York, NY, **1984**.

Seader, J.D.; Henley, E.J. (2006). *Separation Process Principles*, 2nd edition, John Wiley & Sons, Hoboken, NJ,.

Siegel, M., Dwyer, B., Aragon, A., and R. Everett, 2005. *Pilot Demonstrations of Arsenic Treatment Technologies in the U.S. Department of Energy, Arsenic Water Technology Partnership Program, SAND2005-1909C*, Sandia National Laboratories, Albuquerque, NM.

Siegel, M., Marbury, J., Everett, R., Dwyer, B., Collins, S., Aragon, M., and A. Aragon, 2006a, *Pilot Test Specific Test Plan for the Removal of Arsenic from Drinking Water: Socorro, New Mexico, SAND2006-1324*, Sandia National Laboratories, Albuquerque, NM.

Siegel, M., McConnell, P., Everett, R. and K. Kirby, 2006b, *Evaluation of Innovative Arsenic Treatment Technologies: the Arsenic Water Technology Partnership Vendors Forums, Summary Report, SAND2006-5423,* Sandia National Laboratories, Albuquerque, NM.

Siegel, M., Aragon, A., Zhao, H., Everett, R., Aragon, M., Nocon, M., Dwyer, B., Marbury, J., Kirby, C. and K. North, 2007, *Pilot Test of Arsenic Adsorptive Media Treatment Technologies at Socorro Springs, New Mexico, SAND2007-0161*, Sandia National Laboratories, Albuquerque, NM.

Sorensen, M.A., C.B. Koch, M.M. Stackpoole, R.K. Bordia, M.M. Benjamin, T.H. Christensen, 2000a, Effects of thermal treatment on mineralogy and heavy metal behavior in iron oxide stabilized air pollution control residues. *Environmental Science and Technology*; **34**, no.21, p.4620-4627.

Sorensen, MA, M.M. Stackpoole, A.I. Frenkel, R.K. Bordia, G.V. Korshin, T.H. Christensen, 2000b, Aging of iron (Hydr)oxides by heat treatment and effects on heavy metal binding. *Environmental Science and Technology*; **34**(18) 3991-4000.

Sperlich, A., Werner, A., Genza, A., Amy, G., Worch, E.,and M. Jekel, 2005, Breakthrough behavior of granular ferric hydroxide (GFH) fixed-bed adsorption filters: modeling and experimental approaches. *Water Res.*, **39**, 1190–1198.

State of California, 2005, California Code of Regulations (CCR), Title 22, Chapter 11, Article 5, Appendix II.

Thomson, B., Aragon, A., Anderson, J., Chwirka, J., and P. Brady, 2005, *Rapid Small Scale Column Testing for Evaluating Arsenic Adsorbents*, AwwaRF/EPA Report 91074F, 112 p.

US EPA, 1992, Toxicity Characteristic Leaching Procedure. Office of Solid Waste, US Environmental Protection Agency.Washington, DC 20460. http://www.epa.gov/epaoswer/hazwaste/test/pdfs/1311.pdf), last accessed December 22, 2006.

Westerhoff, P., Highfield, D. Badruzzamana, M., and M. Yoon, 2005, Rapid Small-Column Tests for Arsenate Removal in Iron Oxide Packed Columns, *J. Environ. Eng*., **131**, 262-271.

Yoon, R., Salman, T. and G. Donnay, 1979, Predicting zero points of charge of oxides and hydroxides. *Jour. Coll. Interf. Sci.,* **70**, 483-493.

Zouboulis, A.I., and I.A., Katsoyiannis, 2002, Arsenic removal using iron oxide loaded alginate beads, *Ind. Eng. Chem. Res.*, **41**, 6149-6155.

Acknowledgements

The Arsenic Water Technology Partnership (AWTP) program is a multi-year program funded by a Congressional Appropriation through the Department of Energy to develop and test innovative technologies that have the potential to reduce the costs of arsenic removal from drinking water. The AWTP members include Sandia National Laboratories, the American Water Works Association (Awwa) Research Foundation and WERC (A Consortium for Environmental Education and Technology Development). The cooperation and support of members of the Arsenic Water Technology Partnership including Abbas Ghassemi and Rose Thompson (NMSU) and Albert Ilges (AwwaRF) are gratefully acknowledged

The contributions of several coworkers are also gratefully recognized. These include: Randy Everett, Brian Dwyer, Justin Marbury, Richard Kottenstette, Pamela Puissant, Jerome Wright, Emily Wright, Katharine North, (Sandia National Laboratories), Carolyn Kirby (Comforce Technical Services, Inc.), Frederick Partey and Dave Norman (New Mexico Tech). The adsorptive media used in this study were obtained from Graver Technologies, Purolite Company and AdEdge Technologies, Inc.

Sandia is a multiprogram laboratory operated by Sandia Corporation, a Lockheed Martin Company, for the United States Department of Energy's National Nuclear Security Administration under Contract DE-AC04-94AL85000.

This report has been published as Chapter 10, Prediction of Arsenic Removal by Adsorptive Media: Comparison of Field and Laboratory Studies in *Arsenic Contamination of Groundwater: Mechanism, Analysis, and Remediation,* ed. Satinder Ahuja, John Wiley and Sons, Inc, Hoboken, NJ.

APPENDIX 1. EFFECTIVE DIFFUSIVITY IN ADSORBENT PARTICLES

In order to extract the effective diffusivity of arsenic in the macropores of GFH-AD33, a diffusion equation for a macropore-controlled system can be obtained from a differential mass balance on a spherical shell element of the adsorbent particle Ruthven 1984):

$$(1-\varepsilon_p)\frac{\partial q}{\partial t}+\varepsilon_p\frac{\partial c}{\partial t}=\varepsilon_p D_p\left(\frac{\partial^2 c}{\partial R^2}+\frac{2}{R}\frac{\partial c}{\partial R}\right) \tag{1}$$

where $\boldsymbol{\varepsilon_p}$ is adsorbent particle porosity, **q**(R, t) is the adsorbed phase concentration (μg/L of adsorbent), **t** (s) is time, **c** (μg/L) is the adsorbate concentration in the supernate, $\mathbf{D_p}$ (cm^2/s) is the macropore diffusivity of adsorbate in the adsorbent, and **R** (cm) is the radial distance from the center of the adsorbent particle. The macropore diffusivity ($\mathbf{D_p}$) is assume to be independent of concentration in the above equation.

If the adsorption equilibrium is linear (q = Kxc, K is the dimensionless Henry's law adsorption equilibrium constant defined as ratio of adsorbed phase concentration per unit volume of particle (μg/L) to adsorbate concentration (μg/L)), the above equation can be rewritten as:

$$\frac{\partial c}{\partial t}=D_e\left(\frac{\partial^2 c}{\partial R^2}+\frac{2}{R}\frac{\partial c}{\partial R}\right) \tag{2}$$

where $\mathbf{D_e}$ (cm^2/s) is the effective diffusivity defined by:

$$D_e=\frac{\varepsilon_p D_p}{\varepsilon_p+(1-\varepsilon_p)K} \tag{3}$$

The initial and boundary conditions for a step change in the feed and surface concentrations are:

$$\begin{gathered} c(R,0)=c'_0;\ q(R,0)=q'_0 \\ c(R_p,t)=c_0;\ q(R_p,t)=q_0 \\ \left(\frac{\partial c}{\partial R}\right)_{R=0}=\left(\frac{\partial q}{\partial R}\right)_{R=0}=0 \end{gathered} \tag{4}$$

where $\mathbf{R_p}$ (cm) is adsorbent particle radius, $\mathbf{c'_0}$ is the initial adsorbate concentration at a given location **R**, $\mathbf{c_0}$ is the adsorbate concentration at particle surface and at a given time **t**, $\mathbf{q'_0}$ is the initial adsorbed phase concentration at a given location **R**, and is the adsorbed phase concentration at particle surface and at a given time **t** (q_0= K c_0).

The analytical solution for the Equation 8 with the initial and boundary conditions defined by Equation Set 4 is given by Crank (1976) and Ruthven (1984)

$$\frac{\bar{q}-q_0'}{q_0-q_0'}=\frac{M_t}{M_{\max}}=1-\frac{6}{\pi^2}\sum_{n=1}^{\infty}\frac{1}{n^2}\exp\left(-\frac{n^2\pi^2 D_e t}{R_p^2}\right) \tag{5}$$

where $\bar{q}$ **(t)** (μg/L) is the average adsorbed phase concentration through the particle. Where $\mathbf{M_t}$ (μg/L) is the mass gain of adsorbent at time **t**, and $\mathbf{M_{max}}$ (μg/L) is the mass gain of adsorbent at infinite time.

For fractional adsorption uptake $\mathbf{M_t/M_{max}}$ above 70%, Equation (5) can be simplified by using only the first term with a 2% error:

$$\frac{M_t}{M_{\max}} \cong 1 - \frac{6}{\pi^2}\exp\left(\frac{\pi^2 D_e t}{R_p^2}\right) \tag{6}$$

This solution for the fractional adsorption uptake was used to correlate the adsorption kinetics data shown in Figure 4-6. A plot of Ln(1-(M_t/M_{max})) vs. time generates a straight line with a slope of $\left(\frac{-\pi^2 D_e}{R_p^2}\right)$ and an intercept of $Ln\left(\frac{6}{\pi^2}\right)$, from which the effective diffusivity, $\mathbf{D_e}$, for arsenic diffusion in the macropores of the media was calculated. $\left(\frac{D_e}{R_p^2}\right)$ is the diffusion time constant (s^{-1}) that measures the diffusion rate of an adsorbate in the porous media. A large diffusion time constant suggests a slow diffusion rate of adsorbate molecules in the porous media.

APPENDIX 2. RAPID SMALL SCALE COLUMN TESTS

Theory

Laboratory studies to predict media performance of pilot-scale adsorption columns were conducted using rapid small-scale column tests (RSSCTs). RSSCTs are scaled-down columns packed with smaller diameter adsorption media that receive higher hydraulic loading rates to significantly reduce the duration of experiments. Results for RSSCTs can be obtained in a matter of days to a few weeks, whereas pilot tests can take a number of months to over a year.

This method uses scaling relationships that allow correlation of lab-scale column results operated at accelerated flow rates to full-scale column performance. The RSSCT concept is based upon a theoretical analysis of the adsorption processes that govern performance including solution and surface mass transport and adsorption kinetics. Mass transfer models have been used to determine dimensionless parameters that establish similitude between the small- and large-scale columns.

If perfect similitude is maintained, the RSSCTs will have breakthrough profiles that are identical to full-scale columns (Crittenden et al. 1987a). Two mass transfer models are most frequently used to model adsorption columns, the dispersed flow pore and surface diffusion model (DFPSDM) and the homogeneous surface diffusion model (HSDM). The most general model, the DFPSDM, includes pore diffusion and surface diffusion, as well as axial dispersion. This model includes many of the known transport and kinetic phenomena that occur in fixed bed adsorbents; therefore, a dimensional analysis allows the development of scaling factors. The HSDM models surface diffusion while neglecting pore diffusion and axial dispersion. It has been shown that surface diffusion is much greater than pore diffusion for strongly adsorbed species (Hand et al. 1983); therefore, the contribution of pore diffusion to the adsorbate transport has been neglected.

Crittenden et al. (1987a, 1987b, 1991) developed scaling equations for both constant and non-constant diffusivities with respect to particle size. The scaling laws ensure that the RSSCT and the full-scale system will have identical breakthrough profiles. The basis for the RSSCT scaling laws is described below; variables are defined in Tables 1 and 2; definitions of the terms are given in papers cited above.

By equating the modulus of surface diffusivity and assuming equal solute distribution parameters, a relationship between EBCTs for small- and large-scale columns is determined:

$$\frac{EBCT_{SC}}{EBCT_{LC}} = \left[\frac{R_{SC}}{R_{LC}}\right]^2 \frac{D_{s,LC}}{D_{s,SC}} \qquad \text{(Eq. 1)}$$

The dependence of the surface diffusion coefficient on particle radius is defined by the diffusivity factor, x, as follows:

$$\frac{D_{s,SC}}{D_{s,LC}} = \left[\frac{R_{SC}}{R_{LC}}\right]^{x} \qquad \text{(Eq. 2)}$$

Combining these equations yields:

$$\frac{EBCT_{SC}}{EBCT_{LC}} = \left[\frac{R_{SC}}{R_{LC}}\right]^{2-x} \qquad \text{(Eq. 3)}$$

A special case of non-constant diffusivity is a linear relationship between surface diffusivity and particle size (proportional diffusivity, PD). The diffusivity factor, x, becomes equal to one and the ratio of EBCTs becomes:

$$\frac{EBCT_{SC}}{EBCT_{LC}} = \frac{R_{SC}}{R_{LC}} \qquad \text{(Eq. 4)}$$

Table 1. Definition of Terms for RSSCT Scaling Equations

D_s	Surface diffusion coefficient, L^2/T
$EBCT$	Empty bed contact time, T
k_f	Film transfer coefficient, L/T
LC	Subscript denoting large column
R	Particle radius (geometric mean), L
Pe	Peclet number (dimensionless)
Re	Reynolds number (dimensionless)
SC	Subscript denoting small column
Sc	Schmidt number (dimensionless)
x	Diffusivity factor (dimensionless)
ε	Void fraction (dimensionless)
μ	Viscosity of the fluid, M/LT
v	Superficial velocity (hydraulic loading, Darcy velocity), L/T

A minimum value of Re_{SC} is required to establish a minimum velocity that will not over exaggerate the effects of dispersion and external mass transfer. If the small and large columns maintain a constant ratio of their respective Reynolds numbers, the following relation is established:

$$\frac{\mathrm{Re}_{SC,\min}}{\mathrm{Re}_{LC}} = \frac{2v_{SC}R_{SC}/\mu\varepsilon}{2v_{LC}R_{LC}/\mu\varepsilon} \qquad \text{(Eq. 5)}$$

Canceling terms and rearranging gives the ratio of the hydraulic loading of the two columns:

$$\frac{v_{SC}}{v_{LC}} = \frac{R_{LC}}{R_{SC}} \frac{\mathrm{Re}_{SC,\min}}{\mathrm{Re}_{LC}} \qquad \text{(Eq. 6)}$$

Berrigan (1985) showed that dispersion was not important if the product of the Reynolds and Schmidt numbers was in the mechanical dispersion region; therefore, the ratio of hydraulic loadings could be calculated using:

$$\frac{v_{SC}}{v_{LC}} = \frac{R_{LC}}{R_{SC}} \frac{\mathrm{Re}_{SC,\min}\, Sc_{SC}}{\mathrm{Re}_{LC}\, Sc_{LC}} \qquad \text{(Eq. 7)}$$

A requirement for using this equation is that the small-scale column Peclet number (Pe_{SC}) must be greater than or equal to Pe_{LC}; otherwise, a reduction in the hydraulic loading may cause a significant amount of dispersion in the RSSCT.

If the surface diffusivity remains constant with respect to the particle radius (constant diffusivity, CD), then the diffusivity factor, x, is equal to zero and the ratio of EBCTs for small columns and large columns is:

$$\frac{EBCT_{SC}}{EBCT_{LC}} = \left[\frac{R_{SC}}{R_{LC}}\right]^2 \qquad \text{(Eq. 8)}$$

The Stanton and Peclet numbers remain equal between the small scale and full-scale columns only if the surface diffusivity is independent of particle size. If Stanton numbers are identical between process sizes, then the liquid phase mass transfer coefficients can be related to particle radius by:

$$\frac{k_{f,SC}}{k_{f,LC}} = \frac{R_{LC}}{R_{SC}} \qquad \text{(Eq. 9)}$$

If this is the case, the hydraulic loading of the columns is inversely proportional to particle size (Crittenden et al. 1987a):

$$\frac{v_{SC}}{v_{LC}} = \frac{R_{LC}}{R_{SC}} \qquad \text{(Eq. 10)}$$

This relationship will provide equality between Reynolds numbers for both process sizes.

RSSCT Design

The scaling equations discussed above were used to design the RSSCTs. The following input parameters were necessary for further input and design calculations:

- Particle radius, R (cm)
- Column diameter, d (cm)
- Bulk density, ρ (g/mL)
- Pilot empty bed contact time, $EBCT_{pi,lot}$ (min)
- Estimated bed volumes to be processed, BV (--)
- Pilot flow rate, Q (gpm)
- Liquid viscosity, μ (Pa s)
- Liquid density, ρ (kg/m^3)
- Free liquid diffusivity, D_l (m^2/s)
- Bed porosity, ε (--)

Equations used for input and design calculations are shown in Table 2.

Table 2. Input and design calculations for RSSCTs.

Parameter	Pilot	RSSCT (PD)
Column area, A	$\frac{\pi d^2}{4}$	$\frac{\pi d^2}{4}$
EBCT	Input	$EBCT_{pilot}\frac{R_{PD}}{R_{pilot}}$
Hydraulic loading rate, V	$\frac{Q}{A}$	$V_{pilot(m/h)} * \frac{R_{pilot}}{R_{PD}} * \frac{\mathrm{Re}\,Sc_{PD}}{\mathrm{Re}\,Sc_{pilot}}$
Particle diameter, D_p	$R_{pilot} * 2$	$R_{PD} * 2$
Reynolds number, Re	$\frac{\rho V D_p}{\mu \varepsilon}$	$\frac{\rho V D_p}{\mu \varepsilon}$
Schmidt number, Sc	$\frac{\mu}{\rho D_l}$	$\frac{\mu}{\rho D_l}$
Flow rate, Q	$V_{pilot} * A$	$V_{PD} * A$
Bed volume, V_{bed}	$EBCT * Q$	$EBCT * Q$
Bed height, h_{bed}	$\frac{Vol_{bed}}{A}$	$\frac{Vol_{bed}}{A}$
Mass of media, M	$Vol_{bed} * \rho_b$	$Vol_{bed} * \rho_b$
Water required, $L_{req'd}$	$BV * Vol_{bed}$	$BV * Vol_{bed}$
Duration of experiment	$\frac{L_{req'd}}{Q}$	$\frac{L_{req'd}}{Q}$

APPENDIX 3. KLINKENBERG SOLUTION

Modeling Of Adsorption Breakthrough in a Packed Column

A simple mathematical model can be derived from the mass balance of an adsorbent bed element. The partial differential equation governing adsorption breakthrough dynamic behavior can be written as: (Zouboulis et al. 2002; Seader et al. 2006):

$$D_L \frac{\partial^2 c}{\partial z^2} + \frac{\partial (uc)}{\partial z} + \frac{\partial c}{\partial t} + \frac{(1-\varepsilon_b)}{\varepsilon_b}\frac{\partial \bar{q}}{\partial t} = 0 \qquad (1)$$

Where $\mathbf{D_L}$ (cm^2/s) is the axial dispersion coefficient of adsorabte molecules, **z** (cm) is distance coordinate in the flow direction, **c** (μg/L) is the adsorabte (arsenic) concentration, **u** (cm/s) is the interstitial fluid velocity, $\boldsymbol{\varepsilon_b}$ is the porosity of adsorbent bed, **t** (s) is time and $\bar{q}$ (μg/L) is the average adsorbed phased concentration in the adsorbent particle.

Klinkenberg solved the above mass transfer equation and obtained a simple solution for adsorption breakthrough curve based on the following assumptions: (Klinkenberg 1948; Zouboulis et al. 2002; Seader et al. 2006:

(1) Isothermal condition;
(2) No axial dispersion;
(3) Linear driving force for mass transfer;
(4) Linear adsorption equilibrium.

$$\frac{c}{c_F} \approx \frac{1}{2}\left[1 + \mathrm{erf}\left(\sqrt{\tau} - \sqrt{\xi} + \frac{1}{8\sqrt{\tau}} + \frac{1}{8\sqrt{\xi}}\right)\right] \qquad (2)$$

$$\xi = \frac{kKz}{u}\left(\frac{1-\varepsilon_b}{\varepsilon_b}\right) \qquad (3)$$

$$\tau = k\left(t - \frac{z}{u}\right) \qquad (4)$$

$$\bar{q}(t) = \frac{1}{R_p^3}\int_0^{R_p} q(R,t)R^2 dR \qquad (5)$$

$$\frac{\bar{q}}{q_F^*} \approx \frac{1}{2}\left[1 + erf\left(\sqrt{\tau} - \sqrt{\xi} - \frac{1}{8\sqrt{\tau}} - \frac{1}{8\sqrt{\xi}}\right)\right] \qquad (6)$$

where $\mathbf{c_F}$ is the influent adsorbate concentration, τ is the dimensionless time coordinate, ξ is the dimensionless distance coordinate, *k* is the overall mass transfer coefficient (min^{-1}), K is the dimensionless Henry's law adsorption equilibrium constant, where **q(R, t)** (μg/L) is the adsorbed phase concentration inside a spherical adsorbent particle at location **R** and time **t**, $\mathbf{R_P}$ is the adsorbent particle radius, q_F^* (μg/L) is the equilibrium capacity calculated from q_F^* =K c_F.

Equation (2) is an analytical solution of a ratio adsorbate concentration in the fluid phase to that of influent at a given location (**z**) and a given moment (**t**), and equation (6) is an analytical

solution of a ratio adsorbent loading to the equilibrium adsorption amount at a given location (**z**) and a given moment (**t**). If the overall mass transfer coefficient **k** and Henry's constant **K** are known, it is possible to predict:

(1) Adsorption breakthrough curve at bed exit or any location inside the column $\{(C/C_F)$ vs. t$\}$;
(2) Concentration profile inside the column $\{(C/C_F)$ vs. z$\}$ at any time **t**;
(3) Adsorbent loading inside the column $\{(\bar{q}$ vs. z$\}$ at any time.